SAPIENZA
UNIVERSITÀ DI ROMA

Random Path Representation of the Spin O(N) Model

Facoltà di Scienze Matematiche Fisiche e Naturali
Matematica Applicata

Lorenzo Gregoris
ID number 1867373

Advisor
Prof. Lorenzo Taggi

Academic Year 2023/2024

Thesis defended on 23 July 2024
in front of a Board of Examiners composed by:

Prof. M. Manetti (chairman)
Prof. D. Benedetto
Prof. P. Buttà
Prof. G. Nappo
Prof. G. Posta
Prof. V. Silvestri
Prof. A. Teta

Random Path Representation of the Spin O(N) Model
Sapienza University of Rome

This thesis has been typeset by LaTeX and the Sapthesis class.

Author's email: lorenzo.gregoris@gmail.com

Abstract

This thesis introduces a Markov Chain to simulate a random loop soup associated with the Random Path Model (RPM), as presented in [1], which serves as a representation of the classical Spin O(N) model. In the first chapter, we define the classical Spin O(N) model and prove some key results. The second chapter explores expansions of this model, with particular emphasis on the random path representation. In the third chapter, we define the Markov Chain and establish the properties required for its convergence. Finally, the last chapter is dedicated to the simulation of the model, where we present and discuss the results of our numerical experiments.

Keywords: Spin O(N) model, Phase Transitions, Random Path Model, Loop soups, Markov chains, Monte Carlo simulations.

Acknowledgements

This thesis would not have been possible without the support, guidance, and encouragement of many individuals who have contributed to my academic and personal journey.

First and foremost, I would like to express my deepest gratitude to my advisor, Lorenzo Taggi. Thank you for presenting me with such an interesting problem and for all the support you provided in my pursuit of a PhD position, including recommendation letters and invaluable advice.

A special thanks to Chiara Plati, who always kept me informed about exam dates and other crucial information which I should have known. If I smoked, I would have loved doing smoke breaks with you!

I am deeply appreciative of my university friends, who sadly are no longer colleagues: Daniele Lanciotti, who found solace in the peaceful countryside of Porchia; Enrico Massara, who remains immersed in thought instead of playing by the rules and earning his degree; YouYou Lin, who ventured off to steal money from an international organization; and Dr. Paolo Mangini, still crazy enough to pursue studying physics.

The most important thanks goes to my beautiful girlfriend, Elena. Thank you for bearing with me, as I have with you, throughout these years. As I begin my PhD journey in the Netherlands, far from Rome, your support and love mean the world to me. I look forward to our future together, despite the distance.

I also want to express my gratitude to Giulio Ricci. Despite being the furthest member of the *trio* ($\approx$ 1068 km away), your support, especially in these last few months, has been invaluable. Thank you for always being there to talk, answer my questions, and provide suggestions.

I cannot forget my family, especially my parents, who have continued to finance my education. As I prepare to live on my own, I am beginning to fully appreciate all that you have done for me. Please don't throw away the beautiful *vetrinetta* in my room! To my brother, Dado, thank you for letting me use the scooter almost daily. I hope you will soon find your path in life.

A heartfelt thank you to all the people working at the trattoria *Al Biondo Tevere*, for letting me realize how hard a real job can be.

Lastly, but purposefully, I want to thank Jacopo Masia. As the closest member of our *trio* (only $\approx$ 2 km away), you have influenced me to go to the gym more often and guided me through financial investments and taxes. Most importantly, congratulations for achieving the Divine rank in DotA 2 after over 5000 hours of healty dedication!

Thank you all for your unwavering support.

Contents

Introduction

The Spin O(N) model The Ising model, introduced in 1920 by Wilhelm Lenz (who suggested it to his PhD student Ernst Ising), is a deceptively simple yet powerful tool in statistical mechanics for studying magnetism in solids. Despite Ising's demonstration that the one-dimensional model lacks a phase transition, Peierls [2] showed in 1936 that the Ising model in higher dimensions exhibits a richer behavior, namely a spontaneous magnetization phase transition when $d \geq 2$. This has led to a vast field of research in both physics and mathematics, inspiring applications and generalizations in diverse areas like neural networks [3] and algorithmic complexity [4].

This thesis focuses on the classical Spin O(N) model, a generalization of the Ising model introduced by Stanley [5]. This model allows each spin to be a continuous unit N-dimensional vector rather than the binary values of $+1$ and -1 in the Ising model. These spins are typically placed on vertices of a subset of the d-dimensional lattice, and interact with their neighbors, favoring configurations where neighboring spins are aligned (positive inner product), similar to small magnets attracting each other.

While the Ising model ($N = 1$) is well-understood, (Onsager in 1944 solved the two-dimensional Ising model with zero external magnetic field [6]), significant gaps remain in our understanding of continuous spin models ($N \geq 2$).

The Mermin-Wagner theorem shows that unlike the Ising model, no spontaneous magnetization is observed at any finite inverse temperature in two-dimensional models where the single spin space is a compact continuous connected Lie group [7]. However, spontaneous magnetization reappears in three or more dimensions, as established in 1976 by Fröhlich, Simon and Spencer [8] using the powerful methods of infra-red bound and reflection positivity.

Another quantity of interest is the expected value of the inner product of two spins, called spin-spin correlation. In a magnetically ordered phase, this quantity is strictly greater than zero even for spins far away, a phenomenon known as long-range order. This signifies that spins tend to be aligned even over large distances. The high-temperature expansion predicts exponential decay of spin-spin correlations for all these models at high enough temperature. However, the behavior at low temperatures is more complex.

One-dimensional models always exhibit exponential decay of correlations, for higher dimensions, the situation depends on spin dimensionality N and temperature. Understanding the rate of decay of correlations has been a long-standing focus of research, and remains an active area of study. McBryan and Spencer [9] improved on earlier bounds in 1977 by proving that the decay occurs at least at a power-law

rate. For a detailed discussion we refer to [10].

Berezinskii [11], Kosterlitz and Thouless [12] predicted that the XY model ($N = 2$) in two spatial dimensions exhibits power-law decay of correlations at low temperatures. This implies a phase transition from a phase with exponential decay to one with power-law decay, known as the Berezinskii–Kosterlitz–Thouless (BKT) phase transition. The existence of this phase transition was rigorously proven by Fröhlich and Spencer [13]. For two dimensional models and $N \geq 3$, Polyakov [14] predicted in 1975 that that no phase transition occurs and that the spin-spin correlation decays exponentially fast at every positive temperature. As of today, solving this conjecture remains one of the the major open question of the field.

From spins to loops While the Ising model has proven invaluable for studying phase transitions in statistical mechanics, its exact solution becomes increasingly challenging for more complex interactions or higher dimensions. This has led physicists and mathematicians to explore alternative approaches. They started by studying expansions of the partition function in terms of combinatorial objects like subgraphs, walks, loops and integer functions, obtaining new representation of physical systems using intricate geometric structures.

Techniques from probability theory can then be applied to these representations to gain insights into the physical model's properties. For instance, Brydges, Fröhlich and Spencer [15] built upon Symanzik's earlier work [16] to introduce the BFS-random loop model. In this model, closed random walk trajectories interact via local repulsive forces. The spin-spin correlation, when expressed in terms of loops using the BFS-representation, can be understood as the ratio of two partition functions. One partition function corresponding to the weight of configurations with loops and an open path connecting two points, while the other corresponds to configurations with only loops.

A similar approach, used in [1], allowed to prove that with non-zero external magnetic field transverse correlation decay exponentially at all values of the inverse temperature. The model used in this reformulation is called Random Path Model (RPM), and the objects it uses are colored loops (closed paths) and open paths. In the absence of an external magnetic field, this representation becomes a loop soup model, consisting only of closed loops.

While the decay of spin-spin correlations in $d = 2$ implies a vanishing ratio of partition functions, this doesn't directly translate to loops soups models in which only closed loops are allowed. Nonetheless, it is a natural and mathematically interesting question whether a corresponding phase transition can be observed.

It was conjectured in 2011 by Goldschmidt, Ueltschi and Windridgethat [17], that in most cases these loop soups models exhibit a phase with macroscopic loops (their length scales with the size of the system), and the joint distribution of macroscopic loops is always a Poisson-Dirichlet.

This conjecture has been rigorously proven in a model of spatial permutations related to the quantum Bose gas [18], but numerical evidence verified the conjecture in several other models, namely in lattice permutations [19] and in the loop O(N) model [20].

The two-dimensional behaviour of loop soups is different, even though also

interesting and challenging with many unsolved open problems. For example, some loop models, including models of spatial random permutations, are expected to undergo a Berezinskii-Kosterlitz-Thouless phase transition [21].

Existing results by Quitmann and Taggi [22] show that in a general class of random walk loop soup in $d \geq 3$, including the zero-field RPM, there is a phase in which there is a positive density of macroscopic loops. This means that even vertices far away are connected by a loop with uniformly positive probability. In [23] it's also showed that in the regime in which macroscopic loops are present, microscopic and macroscopic loops coexist. Furthermore, in the same article it's proven that, as expected, in the case $d = 2$ (where there is no long range order in the corresponding spin $\mathrm{O}(N)$ model), the probability of two vertices being connected by a loop decays at least algebraically with their distance, at all inverse temperatures.

Outline of the thesis This thesis can be broadly divided into two parts. The first part (Chapters 1 and 2) lays the groundwork by introducing the spin $\mathrm{O}(N)$ model and some of their representation, and discusses relevant established results in the field. The second part (Chapters 3 and 4) presents my modest original contributions, and is focused on the zero-field RPM model.

Chapter 1 introduces the spin $\mathrm{O}(N)$ model on a finite simple graph and briefly presents the DLR formalism for infinite volume measures. We then prove the famous Mermin-Wagner theorem for two-dimensional models and the Spencer-McBryan bound, showing that the decay of spin-spin correlations is at least algebraic.

Chapter 2 is about expansions of the partition function. We first focus on the Ising model ($N = 1$), expanding its partition function using integer-valued functions on edges called currents, and use this expansion to prove that when $d = 1$, there is no spontaneous magnetization at any positive temperature. We then prove using the high-temperature expansion that spin-spin correlations decay exponentially at high enough temperatures whenever $d \geq 2$, and at all finite temperatures in the case $d = 1$. We then adapt the ideas used in the current expansion of the Ising model to obtain a more general representation for the Spin $\mathrm{O}(N)$ model, from which the Random Path Model (RPM) arises. We then briefly explore some applications of this representation, establishing a connection between a specific type of spin-spin correlation and loop events within the RPM.

In **Chapter 3** we define a Markov Chain to study the behavior of the RPM in the case of a two-dimensional square lattice with zero external magnetic field. In this case only closed loops are present, a constraint which makes defining an irreducible Markov Chain non trivial. This task is solved by decomposing the state space into disjoint cycles and then by showing that each cycle can be constructed using a set of simple transformations.

Chapter 4 presents the results obtained through numerical simulations. We begin by providing a concise introduction to Monte Carlo Markov Chains (MCMC), followed by a detailed account of the experimental setup. We then discuss the mixing time of the chain, and analyze some observables, including the mean number of links, the covariance of local times, mean and maximum loop length, and the presence or absence of percolation in the trace of a link configuration.

Chapter 1

The Spin O(N) model

1.1 Definitions

Let $N \geq 1$ be an integer and let $G = (V, E)$ be a finite simple graph. We will denote an edge between vertices x and y by xy. A configuration of the *Spin $O(N)$ model* on G is an assignment $\omega : V \to \mathbb{S}^{N-1}$ of spins to each vertex of G, where $\mathbb{S}^{N-1} \subset \mathbb{R}^N$ is the $(N-1)$-dimensional unit sphere. Different values of N lead to different models, special cases include the Ising model ($N = 1$), in which the single spin state space is simply $\{+1, -1\}$, the XY model ($N = 2$) and the classical Heisenberg model ($N = 3$).

The space of configuration (state space) of the system is $\Omega_G := (\mathbb{S}^{N-1})^V$. At each vertex $x \in V$ we associate the random variable $\varphi_x = (\varphi_x^1, \ldots, \varphi_x^N)$ defined by

$$\varphi_x(\omega) = \omega_x$$

We call *weights* a collection of real numbers $J = (J_e)_{e \in E}$ for each edge of the graph, which will regulate the interaction between neighbouring vertices.

Definition 1.1.1. The *Hamiltonian* of the Spin O(N) model in G with weights $J = (J_e)_{e \in E}$ is defined by

$$\mathcal{H}_{G,N,J}(\omega) := -\sum_{xy \in E} J_{xy} \varphi_x \cdot \varphi_y$$

where $\cdot$ denotes the standard inner product in $\mathbb{R}^N$.

We will only consider *ferromagnetic* weights, that is $J_e \geq 0$ for every edge e. Setting $J_e = 0$ means that there is no interaction between its incident vertices and thus is equivalent to removing e from the edge set. Observe that the Hamiltonian is invariant under simultaneous rotation/reflection of all the spins, reflecting the name of the model.

We define the Gibbs probability measure on G of the Spin O(N) model at inverse temperature $\beta \in \mathbb{R}_{\geq 0}$ and weights J as

$$d\mu_{G,N,\beta}(\omega) := \frac{1}{Z^{spin}_{G,N,J,\beta}} e^{-\beta \mathcal{H}_{G,N,J}(\omega)} d\omega \tag{1.1}$$

where $d\omega := \prod_{x\in V} d\omega_x$ is the product measure having the uniform Lebesgue measure on $\mathbb{S}^{N-1}$ as marginals, and $Z^{spin}_{G,N,\beta}$ is a normalization factor called *partition function*, given by

$$Z^{spin}_{G,N,J,\beta} := \int_{\Omega_G} e^{-\beta\mathcal{H}_{G,N,J}(\omega)} d\omega$$

We denote the expected value of a real valued function of the spin configuration $f : \Omega_G \to \mathbb{R}$, often called an *observable*, with $\langle f\rangle^{spin}_{G,N,J,\beta}$. It will be useful sometimes to consider the not normalized expected value $Z^{spin}_{G,N,J,\beta}[f]$:

$$Z^{spin}_{G,N,J,\beta}[f] := \int_{\Omega_G} f(\omega) e^{-\beta\mathcal{H}_{G,N,J}(\omega)}\, d\omega, \qquad \langle f\rangle^{spin}_{G,N,J,\beta} := \frac{Z^{spin}_{G,N,J,\beta}[f]}{Z^{spin}_{G,N,J,\beta}[1]} \tag{1.2}$$

While the previous definitions work on general finite simple graphs, we will restrict ourselves to finite connected subgraphs of the infinite d-dimensional lattice, denoted by $(\mathbb{Z}^d, \mathbb{E})$. The edge set $\mathbb{E}$ is defined as $\mathbb{E} = \{\{x, y\} \subset \mathbb{Z}^d : \|x-y\|_2 = 1\}$, where $\|\cdot\|_2$ denotes the Euclidean norm, implying that each edge connects nearest neighbors. We assign a weight of $J_e = 1$ to every edge in this lattice, corresponding to the setup often referred to as the *nearest neighbors ferromagnet*.

We adopt the standard notation $\mathbb{Z}^d$ for both the lattice and its vertex set. The *interior boundary* $\partial^{in}G$ and *exterior boundary* $\partial^{ex}G$ of a subgraph $G = (V, E)$ of $\mathbb{Z}^d$ are defined as follows:

$$\partial^{in}G := \{x \in V \,:\, \exists y \in \mathbb{Z}^d \setminus V \text{ such that } \{x, y\} \in \mathbb{E}\}$$
$$\partial^{ex}G := \{x \in \mathbb{Z}^d \setminus V \,:\, \exists y \in V \text{ such that } \{x, y\} \in \mathbb{E}\}$$

i.e. the interior boundary $\partial^{in}G$ consists of vertices in V that are adjacent within the lattice $\mathbb{Z}^d$ to vertices not in V. Conversely, the exterior boundary $\partial^{ex}G$ consists of vertices not in V that are adjacent to vertices in V.

One can break the rotational symmetry of the system by fixing the values of spins on the exterior boundary $\partial^{ex}G$, for example by choosing a direction $\eta \in \mathbb{S}^{N-1}$ and considering the conditioned measure $\mu^{\eta}_{G,N,\beta}(\cdot) := \mu_{G,N,\beta}(\cdot \mid \varphi_x = \eta,\ \forall x \in \partial^{ex}G)$.

Another method to break the symmetry involves introducing an *external magnetic field* $h \in \mathbb{S}^{N-1}$ into the Hamiltonian:

$$\mathcal{H}_{G,N,h}(\omega) := -\sum_{xy\in E} \varphi_x \cdot \varphi_y - \sum_{x\in V} h \cdot \varphi_x$$

Again this can be rewritten using a conditioned measure and by considering a new graph G' with a special added vertex g, called the *ghost* vertex, and adding edges xg for every original vertex $x \in V$. Then, the measure with external field is equivalent to the conditioned measure in which $\varphi_g = h$: $\mu_{G,N,\beta,h}(\cdot) = \mu_{G',N,\beta}(\cdot \mid \varphi_g = h)$.

1.2 Phase Transitions and the DLR Formalism

We are interested in the behaviour of this model as a function of the inverse temperature β, as the size of the system goes to infinity–the *thermodynamic limit*. Considering an infinite system is a necessity if we want to obtain the singular

behaviour of macroscopic properties associated with phase transitions: any finite volume measure (1.1) is an analytic function of the inverse temperature β.

In this limit the notion of Hamiltonian loses its meaning: one must consider instead the limit of the expectations (1.2). More precisely, given a suitable sequence of finite graphs G_n converging to $\mathbb{Z}^d$, we are interested in the weak limit of the measures $\mu_{G_n,\beta}$ denoted by μ_β, if it exists. For $N = 1, 2$, using correlation inequalities it's possible to prove that given any local function $f : \mathbb{Z}^d \to \mathbb{R}$, the limit $\lim_{n\to\infty}\langle f\rangle_{G_n,\beta}$ exists.
An alternative approach was introduced by Dobrushin, Lanford and Ruelle [24, 25], in which the infinite volume measure is not obtained by a limiting procedure, but by requiring a certain consistency condition: the infinite-volume probability measure describe equilibrium in the full space: each finite volume must be in equilibrium with the whole, hence, the finite-volume prescriptions must be weighted by the full-volume prescription. This leads to the definition that μ, is a infinite volume Gibbs measure (for a given interaction and inverse temperature) if

$$\langle f\rangle_\beta = \int_\Omega f(\omega)\,\mu(d\omega) = \int_\Omega \langle f\rangle^\eta_{\Lambda,\beta}\,\mu(d\eta) \tag{1.3}$$

for each observable f. These are the celebrated DLR equations (for Dobrushin, Lanford and Ruelle). From a more probabilistic perspective, this formula means that the conditional expectation of μ on the finite region Λ given the outside configuration η_{Λ^c} coincides with the Boltzmann-Gibbs average.

Thus, infinite volume Gibbs measures are defined in terms of their conditional distributions. The richness of statistical mechanics comes from the fact that, unlike marginal distributions (Kolmogorov extension theorem), conditional distributions do not necessarily determine a measure uniquely. We denote the set of all infinite volume Gibbs measures for the spin O(N) model as $\mathcal{G}(N)$. It is established that at least one infinite volume Gibbs measure exists, i.e., $\mathcal{G}(N) \neq \emptyset$, but there may be more than one $|\mathcal{G}(N)| > 1$: in this case, we are in the presence of a first-order phase transition.

The existence of at least one such measure, follows from *quasilocality* of the interaction and the *sequential compactness* of the space of measures on $\Omega_{\mathbb{Z}^d}$. Quasilocality ensures that the finite-volume expected value of f is weakly dependent on the boundary conditions as long as the system size is sufficiently large to separate the support of the local function f from the boundary. In our case, with nearest-neighbor interaction, this is trivially satisfied (we in fact have *locality*). Sequential compactness of the space of measures on $\Omega_{\mathbb{Z}^d}$ guarantees the existence of a converging subsequence. This allows us to construct infinite volume Gibbs measures by taking limits of finite volume measures. For instance, consider a boundary condition $\eta \in \Omega$ and the sequence of finite subgraphs $B_n := \{-n, \dots, n\}^d$, and define measures

$$\mu_n(\omega) := \begin{cases} \mu^\eta_{B_n,\beta}(\omega) & \text{if } \omega_{B_n{}^c} = \eta_{B_n{}^c}, \\ 0 & \text{otherwise.} \end{cases}$$

With the σ-algebra generated by cylinders sets,

$$\mathcal{A}_n = \sigma(\mathcal{C}(B_n)), \qquad \mathcal{C}(B_n) := \{\Pi^{-1}_{B_n}(E) \,:\, E \in \mathcal{B}(\Omega_{B_n})\}$$

where $\Pi_{B_n}^{-1}$ is the preimage of the projection map on B_n, and $\mathcal{B}$ is the Borel σ-algebra[1].

Then, this sequence of probability measures on $\Omega_{\mathbb{Z}^d}$ admits a converging subsequence to an infinite volume measure μ^η that satisfies the DLR equations, with the σ-algebra $\sigma(\mathcal{C}(\mathbb{Z}^d))$. We denote the expected value with respect to these measures with $\langle\cdot\rangle_\mu^\eta$. If uniqueness holds, then every boundary condition η yields the same infinite volume measure. Conversely, different boundary conditions may lead to distinct measures.

In practice, calculating finite volume measures with a chosen boundary condition and examining their limits as the volume grows, provides a way to study properties of infinite volume measures, and is the only way one can employ computational techniques to obtain estimates. For a more detailed exposition, we refer to [26, Ch. 6].

With the introduction of an infinite volume measure, we can now investigate how these models behave in relation to these standard properties:

- The model exhibits *spontaneous magnetization* at β if
$$\langle\varphi_0 \cdot \eta\rangle_\mu^\eta > 0 \qquad (\text{MAG}_\beta).$$
- The model exhibits *long-range ordering* at β if
$$\lim_{\|x\|\to\infty} \langle\varphi_0 \cdot \varphi_x\rangle_\mu > 0 \qquad (\text{LRO}_\beta).$$
- The model exhibits *exponential decay of correlations* at β if there exists $c_\beta > 0$ such that
$$\langle\varphi_0 \cdot \varphi_x\rangle_\mu \leq e^{-c_\beta\|x\|} \text{ for all x } \in \mathbb{Z}^d \qquad (\text{EXP}_\beta).$$

These properties lead to critical parameters separating phases where these phenomena either occur or not

$$\begin{aligned}\beta_{\text{mag}}^c &:= \inf\{\beta > 0 : (\text{MAG}_\beta)\},\\ \beta_{\text{lro}}^c &:= \inf\{\beta > 0 : (\text{LRO}_\beta)\},\\ \beta_{\text{exp}}^c &:= \sup\{\beta > 0 : (\text{EXP}_\beta)\}.\end{aligned}$$

Using the high temperature expansion, we will prove in Section 2.2 that all these models exhibit exponential decay of correlation at sufficiently low, but non-zero, inverse temperature. In particular, one-dimensional models always show exponential decay of correlations, i.e. $\beta_{exp}^c = \infty$.

In Section 2.1 we will prove that the one-dimensional Ising model ($N = 1$) does not exhibit spontaneous magnetization ($\beta_{mag}^c = \infty$). Peierls [2] proved that the Ising model with dimension $d \geq 2$ possesses a non trivial critical inverse temperature $\beta_{mag}^c < \infty$ using his famous argument.

The same is true for continuous spins ($N \geq 2$) and dimension of the lattice $d \geq 3$, as proved by Fröhlich and Spencer [8]. However, perhaps surprisingly, spontaneous

[1] Ω_{B_n} is equipped with the product topology, and each site $\mathbb{S}^{N-1}$ with the the topology inherited from the embedding $\mathbb{S}^{N-1} \subset \mathbb{R}^N$.

magnetization is absent in two-dimensional models, a consequence of the Mermin-Wagner theorem [7]. This theorem, which we will discuss in detail and prove in Section 1.3, states that the infinite volume Gibbs measures of a model on $\mathbb{Z}^2$, with local interactions and where the single-spin space is invariant with respect to a compact continuous connected Lie group, are rotationally invariant. This implies that no magnetization is present: $\beta_{mag}^c = +\infty$. Then, two scenarios are possible:

- $\beta_{\text{exp}}^c = \infty$: the model does not undergo any phase transition. This behavior was predicted by Polyakov [14] for planar O(N) models with $N \geq 3$.
- $\beta_{\text{exp}}^c < \infty$: the model undergoes a Berezinsky-Kosterlitz-Thouless (BKT) phase transition. This type of transition is named after Berezinskii [11] and Kosterlitz-Thouless [12], who independently introduced it for the planar XY-model (albeit non-rigorously). The existence of this transition was later proven mathematically by Fröhlich and Spencer [13].

For two-dimensional models, the decay of correlation is at least algebraic, as shown by McBryan and Spencer [9]. This result will be proven in Section 1.4.

The current state of knowledge for these models is summarized in Table 1.1. As of today, the $N \geq 3$ case remains open and represent an active area of research.

O(N)	**d = 2**	**d ≥ 3**
N = 1 (Ising)	Continuous sharp order-disorder	
N = 2	BKT	Sharp order-disorder
N ≥ 3	No phase transitions?	Sharp order-disorder

Table 1.1. Phase transitions in the spin O(N) model.

1.3 The Mermin-Wagner theorem

The Hamiltonian of the spin O(N) model (1.1.1) is invariant with respect to global rotations. Given an element $r \in \text{SO}(N)$ and a configuration $\omega \in \Omega$, a global rotation is defined as the rotation of each spin:

$$(r\omega)_x := r\omega_x, \quad \forall x \in \mathbb{Z}^d.$$

The effect of a global rotation on events $A \in \mathcal{F}$ is defined by $rA := \{r\omega : \omega \in A\}$, and on probability measures by

$$r\mu(A) := \mu(r^{-1}A).$$

This symmetry of the Hamiltonian implies that the set of infinite volume Gibbs measures $\mathcal{G}(N)$ is also invariant, meaning it is closed with respect to global rotations: if $\mu \in \mathcal{G}(N)$, then $r\mu \in \mathcal{G}(N)$. The Mermin-Wagner theorem shows further that when $d = 1$ or 2, $r\mu = \mu$ for all $r \in \text{SO}(N)$.

In the following sections we use the notation $\langle\cdot\rangle_\mu$ to denote the expected value with respect to an infinite volume Gibbs measure $\mu \in \mathcal{G}(N)$.

Theorem 1.3.1 (Mermin-Wagner)**.** Let $N \geq 2$. Then, when $d = 1$ or 2, all infinite-volume Gibbs measures are invariant under the action of $\mathrm{SO}(N)$: for all $\mu \in \mathcal{G}(N)$,

$$r\mu = \mu, \quad \forall r \in \mathrm{SO}(N).$$

A direct consequence of theorem 1.3.1 is that in an infinite system whose equilibrium properties are described by a Gibbs measure $\mu \in \mathcal{G}(N)$, the distribution of each individual spin φ_i is uniform on $\mathbb{S}^{N-1}$: given any measurable set $A \subseteq \mathbb{S}^{N-1}$, and an element $r \in \mathrm{SO}(N)$,

$$\mu(\varphi_i \in A) = r\mu(\varphi_i \in A) = \mu(\varphi_i \in r^{-1}A).$$

which implies that spontaneous magnetization cannot be observed in one or two-dimensional systems with continuous symmetries, even at very low temperature ($\beta^c_{mag} = +\infty$)

$$\langle \varphi_0 \rangle_\mu = \mathbf{0}, \qquad d = 1, 2, \quad N \geq 2. \tag{1.4}$$

The $\mathrm{SO}(N)$-invariance of the infinite-volume Gibbs measures also implies the absence of orientational long-range order: $\beta^c_{lro} = +\infty$. Fix $k \in \mathbb{Z}^d$, and let n be large, but small enough to have $k \in B^c_n$. If $\mu \in \mathcal{G}(N)$, then by the DLR compatibility conditions,

$$\langle \varphi_0 \cdot \varphi_k \rangle_\mu = \int \langle \varphi_0 \cdot \varphi_k \rangle^\eta_{B_n,\beta} \mu(d\eta) = \int \langle \varphi_0 \rangle^\eta_{B_n,\beta} \cdot \varphi_k(\eta) \mu(d\eta).$$

We will obtain a quantitative version of (1.4) in the proof of theorem 1.3.1, a consequence of which will be that $\lim_{n\to\infty} \langle \varphi_0 \rangle^\eta_{B_n,\beta} = 0$, uniformly in the boundary condition η. Therefore, by dominated convergence,

$$\langle \varphi_0 \cdot \varphi_k \rangle_\mu \to 0 \text{ when } \|k\|_\infty \to \infty.$$

Before starting the proof, we introduce some notation and results for harmonic functions on the lattice which we will need to optimize some functionals.

Harmonic Functions on the Lattice

For this section we consider a connected subgraph $G = (V, E)$ of $\mathbb{Z}^d$, in which each vertex in the interior has degree $2d$. Furthermore each edge occurs with both orientations; for an edge pointing from vertex x to vertex y, denoted by xy, we define $e^- = x$ and $e^+ = y$. We focus on a specific category of vertex functions that enjoy an averaging property.

Definition 1.3.1 (Harmonic function)**.** A vertex function $u : V \to \mathbb{R}$ is *harmonic* on $W \subseteq V$ if

$$u(x) = \frac{1}{2d} \sum_{y \sim x} u(y), \qquad \forall x \in W$$

where $y \sim x$ denotes that y is adjacent to x.

Harmonic functions satisfy a *maximum principle*, that is, if the supremum of u is attained in a vertex $\overline{x} \in W$, then u is constant [27, Ch. 2.1]. This observation leads to a *uniqueness principle*: if $f, g : V \to \mathbb{R}$ are both harmonic on a finite set W, and agree outside, $f(x) = g(x)$ for all $x \notin W$, then $f = g$ (consider the harmonic function $h := f - g$).

Following standard notation, we refer to these harmonic functions as voltage functions. Imagine placing unit resistors on each edge of the lattice, then along each edge there is a current

$$i(xy) := v(x) - v(y) \tag{1.5}$$

where v is an harmonic function on the set $(A \cup Z)^c$, with $A \cap Z = \emptyset$, and with fixed values $v \equiv v_A$ on A and $v \equiv 0$ on Z (the vertices in A are hooked to a battery of potential v_A, those in Z are grounded). Define $l^2(V)$ to be the real Hilbert space of functions on V with the inner product

$$(f, g) := \sum_{x \in V} f(x)g(x).$$

Define $l^2_-(E)$ to be the space of antisymmetric functions θ on E, that is, $\theta(-e) = -\theta(e)$ for each edge e) with the inner product

$$(\theta, \theta') := \frac{1}{2} \sum_{e \in E} \theta(e)\theta'(e) = \sum_{e \in E_{1/2}} \theta(e)\theta'(e), \tag{1.6}$$

where $E_{1/2} \subset E$ is a set of edges containing exactly one of each pair $e, -e$. Note that the current (1.5) belongs to this space. Define the *coboundary operator* $\nabla : l^2(V) \to l^2_-(E)$ by

$$(\nabla f)(e) := f(e_-) - f(e_+).$$

Conversely, given an antisymmetric function on the edges, we are interested in the net flow out of a vertex, whence we define the *boundary operator* $\nabla^* : l^2_-(E) \to l^2(V)$ by

$$(\nabla^* \theta)(x) := \sum_{e^- = x} \theta(e).$$

We use the superscript $*$ because these two operators are adjoints of each other:

$$\forall f \in l^2(V), \forall \theta \in l^2_-(E) \quad (\theta, \nabla f) = (\nabla^* \theta, f).$$

We further define the *discrete Laplacian operator* Δ as

$$\Delta f(x) := \frac{1}{2d} \nabla^* \nabla f(x) = \frac{1}{2d} \sum_{y \sim x} f(y) - f(x)$$

Note that f is harmonic at x iff $\Delta f(x) = 0$.
Using the coboundary operator, the definition of a current (Ohm's Law) can be written as

$$i(e) := (\nabla v)(e)$$

We see that *Kirchhoff node law* holds for the current, since

$$\nabla^* i(x) = \nabla^* \nabla v(x) = 2d \Delta v(x) \tag{1.7}$$

and if $x \notin A \cup Z$, then the right term is zero since v is harmonic at x. From this follows immediately a general fact. Denote by $\text{Strenght}(i)$ the total amount of current flowing into the circuit

$$\text{Strenght}(i) := \sum_{x \in A} \nabla^* i(x)$$

Proposition 1.3.1. Given any vertex function $f : V \to \mathbb{R}$ such that $f \equiv \alpha$ on A and $f \equiv 0$ on Z, we have

$$(\nabla f, i) = \alpha \text{Strenght}(i) \tag{1.8}$$

Proof. By (1.7)

$$(\nabla f, i) = (f, \nabla^* i) = \sum_{x \in A} \nabla^* i(x) = \alpha \sum_{x \in A} \nabla^* i(x) = \alpha \text{Strenght}(i)$$

□

The quantity $\text{Strenght}(i)$ is related to the *escape probability* of the symmetric random walk $(X_n)_{n \geq 0}$. Given a subset $C \subseteq V$, define the stopping times

$$\tau_C := \inf\{n \geq 0 \, : \, X_n \in C\}$$
$$\tau_C^+ := \inf\{n \geq 1 \, : \, X_n \in C\}$$

Let $A, Z \subset V$ be two disjoint subsets, and identify all vertices in A with a single vertex a. The escape probability from A to Z is defined as

$$P[A \to Z] := P_a[\tau_Z < \tau_a^+]$$

that is, starting from a, the probability of reaching the set Z before returning to a. Let $u(x) := P_x[\tau_a < \tau_Z]$, then

$$P[A \to Z] = \sum_{a \in A} \sum_{x \sim a} \frac{1}{2d}(1 - u(x)) = \frac{1}{2d} \sum_{a \in A} \sum_{x \sim a} i(ax) = \frac{1}{2d} \text{Strength}(i)$$

Escape probability is related to recurrence of the random walk. Consider the sequence of subgraphs $(B_n)_{n \geq 1}$, which satisfies $B_n \subseteq B_{n+1}$ and $\cup_n B_n = \mathbb{Z}^d$, and identify all vertices outside B_n in a single vertex z_n. Now for every $a \in \mathbb{Z}^d$, the events $\{a \to z_n\}$ are decreasing, so by continuity of measures

$$P[\bigcap_{n \geq 0} \{a \to z_n\}] = \lim_{n \to \infty} P[a \to z_n]$$

is the probability of never returning to a. This is positive iff the random walk on $\mathbb{Z}^d$ is transient. But in dimension one and two, the symmetric random walk is recurrent, which implies that the strength of the current goes to zero. In our case, $A = B_\ell$ and $Z = B_n^c$. We will give an upper bound on how fast this quantity goes to zero in n, uniformly in ℓ, using a form of the Nash-Williams Inequality [27, Ch. 2.5] specialized in our setting. A set Π of edges separates A and Z if every path with one endpoint in A and the other endpoint in Z must include an edge in Π; These edge subsets are called *cutsets*.

Theorem 1.3.2 (Nash–Williams inequality)**.** Let A, Z be two disjoint subsets in a finite graph that are separated by pairwise disjoint cutsets $\Pi_1, \dots, \Pi_n$, let $i = \nabla v$ where v is the potential with $v_A = 1$ and $v_Z = 0$, then

$$\text{Strength}(i) \le \left(\sum_{k \ge 1} \frac{1}{|\Pi_k|} \right)^{-1}$$

Proof. Since Π_k are cutsets, from flow conservation $\sum_{e \in \Pi_k} |i(e)| \ge \text{Strength}(i)$. Then using Cauchy–Schwarz

$$\sum_{e \in \Pi_k} i(e)^2 |\Pi_k| = \sum_{e \in \Pi_k} i(e)^2 \sum_{e \in \Pi_k} 1 \ge \left(\sum_{e \in \Pi_k} |i(e)| \right)^2 \ge \text{Strength}(i)^2$$

so that

$$\text{Strength}(i) \ge \sum_k \sum_{e \in \Pi_k} i(e)^2 \ge \text{Strength}(i)^2 \sum_k \frac{1}{|\Pi_k|}$$

□

We can easily find a sequence of $n - \ell$ cutsets when $A = B_\ell$ and $Z = B_n^c$. In the one and two dimensional case we obtain the following bounds:

$$\text{Strength}(i) \le \begin{cases} 2/(n-\ell) & \text{for } d = 1, \\ 8/\log\left(\dfrac{n}{\ell+1}\right) & \text{for } d = 2. \end{cases} \tag{1.9}$$

Proof of Theorem for the Case N = 2

Returning to Theorem (1.3.1), we first give a proof of the result in the case $N = 2$, and then use it to address the general case. We write $\varphi_i = (\cos\theta_i, \sin\theta_i)$ and set $V(\theta) := \cos(\theta)$.

Let $\mu \in \mathcal{G}(2)$ and let $r_\psi \in \text{SO}(2)$ denote the rotation of angle $\psi \in (-\pi, \pi]$. To show that $r_\psi \mu = \mu$, we shall show that $\langle f \rangle_\mu = \langle r_\psi f \rangle_\mu$ for each local bounded measurable function f. Since the characteristic function of a cylinder set is a local function, and cylinder sets are a π-system, the previous equality implies $\mu = r\mu$. By the DLR compatibility conditions (1.3), we can write, for any finite $\Lambda \subset \mathbb{Z}^d$,

$$|\langle f \rangle_\mu - \langle r_\psi f \rangle_\mu| \le \int |\langle f \rangle^\eta_{\Lambda,\beta} - \langle r_\psi f \rangle^\eta_{\Lambda,\beta}| \, \mu(d\eta). \tag{1.10}$$

We study the differences $|\langle f \rangle^\eta_{\Lambda,\beta} - \langle r_\psi f \rangle^\eta_{\Lambda,\beta}|$ quantitatively in the following proposition, from which the Mermin-Wagner theorem follows.

Proposition 1.3.2. Assume that $d = 1$ or $d = 2$ and fix $N = 2$. Under the hypotheses of Theorem 1.3.1, there exist constants c_1, c_2 such that, for any boundary condition $\eta \in \Omega$, any inverse temperature $\beta < \infty$, any angle $\psi \in (-\pi, \pi]$ and any $\ell \in \mathbb{Z}_{\ge 0}$,

$$|\langle f \rangle^\eta_{B_n;\beta} - \langle r_\psi f \rangle^\eta_{B_n;\beta}| \le \beta^{1/2} |\psi| \|f\|_\infty \times \begin{cases} c_1/(n-\ell)^{1/2} & \text{if } d = 1, \\ c_2/\left(\log \frac{n}{(\ell+1)}\right)^{1/2} & \text{if } d = 2, \end{cases}$$

for all $n > \ell$ and all bounded functions f such that $\text{supp}(f) \subset B_\ell$.

Most of the proof of the bounds does not depend on the shape of the system considered. So, let us first consider an arbitrary connected Λ, which will later be taken to be the box B_n.
We start by express rewriting

$$\langle r_\psi f\rangle^\eta_{\Lambda,\beta} = (Z^\eta_{\Lambda,\beta})^{-1}\int f(r_{-\psi}\omega)e^{-\mathcal{H}_{\Lambda,\beta}(\omega_\Lambda\eta_{\Lambda^c})}\prod_{x\in\Lambda}d\omega_x$$

as the expectation of f under a modified distribution. We let Λ and ℓ be large enough so that $\Lambda \supset B_\ell \supset \mathrm{supp}(f)$.

Let $\Psi : \mathbb{Z}^d \to (-\pi,\pi]$ satisfy $\Psi_x = \psi$ for all $x \in B_\ell$, and $\Psi_x = 0$ for all $x \notin \Lambda$. An explicit choice for Ψ will be made later. Let $t_\Psi : \Omega \to \Omega$ denote the transformation under which

$$\theta_x(t_\Psi\omega) = \theta_x(\omega) + \Psi_x, \forall\omega\in\Omega.$$

That is, t_Ψ acts as the identity on spins located outside Λ and as the rotation r_ψ on spins located inside B_ℓ. Observe that $t_{-\Psi} = t_\Psi^{-1}$. Now, since $t_{-\Psi}\omega$ and $r_{-\psi}\omega$ coincide on $\mathrm{supp}(f) \subset B_\ell$,

$$\begin{aligned}\int f(r_{-\psi}\omega)e^{-\mathcal{H}_{\Lambda,\beta}(\omega_\Lambda\eta_{\Lambda^c})}\prod_{x\in\Lambda}d\omega_x &= \int f(t_{-\Psi}\omega)e^{-\mathcal{H}_{\Lambda,\beta}(\omega_\Lambda\eta_{\Lambda^c})}\prod_{x\in\Lambda}d\omega_x\\ &= \int f(\omega)e^{-\mathcal{H}_{\Lambda,\beta}(t_\Psi(\omega_\Lambda\eta_{\Lambda^c}))}\prod_{x\in\Lambda}d\omega_x.\end{aligned}$$

In the second equality, we used the fact that the mapping $\omega_\Lambda \mapsto (t_{-\Psi}\omega)_\Lambda$ has a Jacobian equal to 1. Let $\langle\cdot\rangle^{\eta,\Psi}_{\Lambda,\beta}$ denote the expectation under the probability measure

$$\mu^{\eta,\Psi}_{\Lambda,\beta}(A) = (Z^{\eta,\Psi}_{\Lambda,\beta})^{-1}\int_{\Omega_\Lambda} e^{-\mathcal{H}_{\Lambda,\beta}(t_\Psi(\omega_\Lambda\eta_{\Lambda^c}))}1_A(\omega_\Lambda\eta_{\Lambda^c})\prod_{x\in\Lambda}d\omega_x,\quad A\in\mathcal{F}.$$

Observe that, for the same reasons as above (the Jacobian being equal to 1 and the boundary condition being preserved by t_Ψ), the partition function is actually left unchanged:

$$Z^{\eta,\Psi}_{\Lambda,\beta} = Z^\eta_{\Lambda,\beta}.$$

We can then write $\langle r_\psi f\rangle^\eta_{\Lambda,\beta} = \langle f\rangle^{\eta,\Psi}_{\Lambda,\beta}$, and therefore

$$|\langle f\rangle^\eta_{\Lambda,\beta} - \langle r_\psi f\rangle^\eta_{\Lambda,\beta}| = |\langle f\rangle^\eta_{\Lambda,\beta} - \langle f\rangle^{\eta,\Psi}_{\Lambda,\beta}|,$$

which reduces the problem to comparing the expectation of f under the measures $\mu^\eta_{\Lambda,\beta}$ and $\mu^{\eta,\Psi}_{\Lambda,\beta}$.

One convenient way of measuring the "closeness" of two measures μ,ν is the relative entropy

$$h(\mu|\nu) = \begin{cases}\left\langle \frac{d\mu}{d\nu}\log\frac{d\mu}{d\nu}\right\rangle_\nu & \text{if } \mu \ll \nu,\\ \infty & \text{otherwise,}\end{cases}$$

where $\frac{d\mu}{d\nu}$ is the Radon–Nikodym derivative of μ with respect to ν. Particularly well-suited to our needs is Pinsker's inequality [26, Lemma B.67], which states that, for any measurable function f with $\|f\|_\infty \le 1$,

$$|\langle f\rangle_\mu - \langle f\rangle_\nu| \le \sqrt{2h(\mu|\nu)}. \tag{1.11}$$

In our case,

$$\frac{d\mu^{\eta}_{\Lambda,\beta}}{d\mu^{\eta,\Psi}_{\Lambda,\beta}}(\omega) = e^{\mathcal{H}_{\Lambda,\beta}(t_\Psi\omega)-\mathcal{H}_{\Lambda,\beta}(\omega)}.$$

Using Pinsker's inequality,

$$\begin{aligned}|\langle f\rangle^{\eta}_{\Lambda,\beta} - \langle f\rangle^{\eta,\Psi}_{\Lambda,\beta}| &\le \|f\|_\infty\sqrt{2h(\mu^{\eta}_{\Lambda,\beta}|\mu^{\eta,\Psi}_{\Lambda,\beta})} \\ &= \|f\|_\infty\sqrt{2\left\langle \mathcal{H}_{\Lambda,\beta}\circ t_\Psi - \mathcal{H}_{\Lambda,\beta}\right\rangle^{\eta}_{\Lambda,\beta}}.\end{aligned}$$

A second-order Taylor expansion yields

$$\begin{aligned}\left\langle \mathcal{H}_{\Lambda,\beta}\circ t_\Psi - \mathcal{H}_{\Lambda,\beta}\right\rangle^{\eta}_{\Lambda,\beta} &= \beta\sum_{xy\in E_\Lambda}\langle V(\theta_y-\theta_x+\Psi_y-\Psi_x)-V(\theta_y-\theta_x)\rangle^{\eta}_{\Lambda,\beta} \\ &\le \beta\sum_{xy\in E_\Lambda}\left(\langle V'(\theta_y-\theta_x)\rangle^{\eta}_{\Lambda,\beta}(\Psi_y-\Psi_x)+\frac{C}{2}(\Psi_y-\Psi_x)^2\right).\end{aligned}$$

We now get rid of the first order terms using the following trick: since the relative entropy is always non-negative, we can write

$$h(\mu^{\eta}_{\Lambda,\beta}|\mu^{\eta,\Psi}_{\Lambda,\beta}) \le h(\mu^{\eta}_{\Lambda,\beta}|\mu^{\eta,\Psi}_{\Lambda,\beta}) + h(\mu^{\eta}_{\Lambda,\beta}|\mu^{\eta,-\Psi}_{\Lambda,\beta}).$$

The second term in the right-hand side of the latter expression can be treated as above, and gives rise to the same first-order terms but with the opposite sign. These thus cancel, and we are left with

$$h(\mu^{\eta}_{\Lambda,\beta}|\mu^{\eta,\Psi}_{\Lambda,\beta}) \le C\beta\sum_{e\in E_\Lambda}(\nabla\Psi^2)_e. \tag{1.12}$$

Our task is to find a vertex function Ψ that minimizes the previous sum, called energy, with boundary conditions $\Psi(x)=0$ on Λ^c and $\Psi(x)=\psi$ on B_ℓ. We make a small detour and consider the general minimization problem:

$$\mathscr{E}(\Psi) := \frac{1}{2}\sum_{e\in E_\Lambda}(\nabla\Psi)^2_e, \qquad \Psi_x=\Psi_A \quad \forall x\in A, \quad \Psi_x=0 \quad \forall x\in Z, \tag{1.13}$$

where A and Z are two disjoint subsets of vertices. Also, the energy can be written using the inner product (1.6):

$$\mathscr{E}(\Psi) = \frac{1}{2}(\nabla\Psi,\nabla\Psi) = \frac{1}{2}\|\nabla\Psi\|^2 \tag{1.14}$$

Lemma 1.3.1. The Dirichlet energy (1.14) possesses a unique minimizer among all functions $u:\mathbb{Z}^d\to\mathbb{R}$ satisfying $u(x)=0$ for all $x\notin\Lambda$, and $u(x)=1$ for all $x\in B_\ell$, given by the probabilities

$$u^*(x) = P_x(\tau_{B_\ell}<\tau_\Lambda), \tag{1.15}$$

where P_x is the law of the simple random walk on $\mathbb{Z}^d$ started at x. Moreover,

$$\mathscr{E}(u^*) = \frac{1}{2}\text{Strength}(i), \qquad \text{where } i=\nabla u^*$$

Proof. Let us first characterize the critical points of $\mathscr{E}$. Assume u is a critical point satisfying the constraints. Then we must have

$$\frac{d}{ds}\mathscr{E}(u+s\xi)\Big|_{s=0} = 0,$$

for all perturbations $\xi : \mathbb{Z}^d \to \mathbb{R}$ such that $\xi(x) = 0$ for all $x \notin \Lambda \setminus B_\ell$. A simple computation yields

$$\frac{d}{ds}\mathscr{E}(u+s\xi)\Big|_{s=0} = (\nabla u, \nabla \xi) = 2d(\Delta u, \xi)$$

this implies that u is harmonic in $\Lambda \setminus B_\ell$. Then u is a voltage function with $A = B_\ell$ and $Z = \Lambda^c$. We now show that u^* is in fact the minimizer. Let $i := \nabla u^*$, then

$$0 \leq \|\nabla u - i\|^2 = (\nabla u - i, \nabla u - i) = \|\nabla u\|^2 + \|i\|^2 - 2(\nabla u, i)$$

using Proposition (1.8) to rewrite the last term and that $u = 1$ on A we find

$$\|i\|^2 \leq \|\nabla u\|^2$$

The value attained at the minimum is

$$\mathscr{E}(u^*) = \frac{1}{2}\|i\|^2 = \frac{1}{2}(\nabla u, i) = \frac{1}{2}(u, \nabla^* i) = \frac{1}{2}\text{Strength}(i)$$

The function (1.15) trivially satisfies the boundary values, since $u \equiv 1$ in A and $u \equiv 0$ in Z, and is harmonic in $(A \cup Z)^c$:

$$u(x) = \sum_{y\sim x} P_x[\text{ first step is to y}]P_x[\tau_A < \tau_Z \mid \text{ first step is to y}] = \sum_{x\sim y} \frac{1}{2d}u(y) \tag{1.16}$$

and is thus the unique solution, since the minimizer is an harmonic function on a finite domain with fixed boundary conditions. □

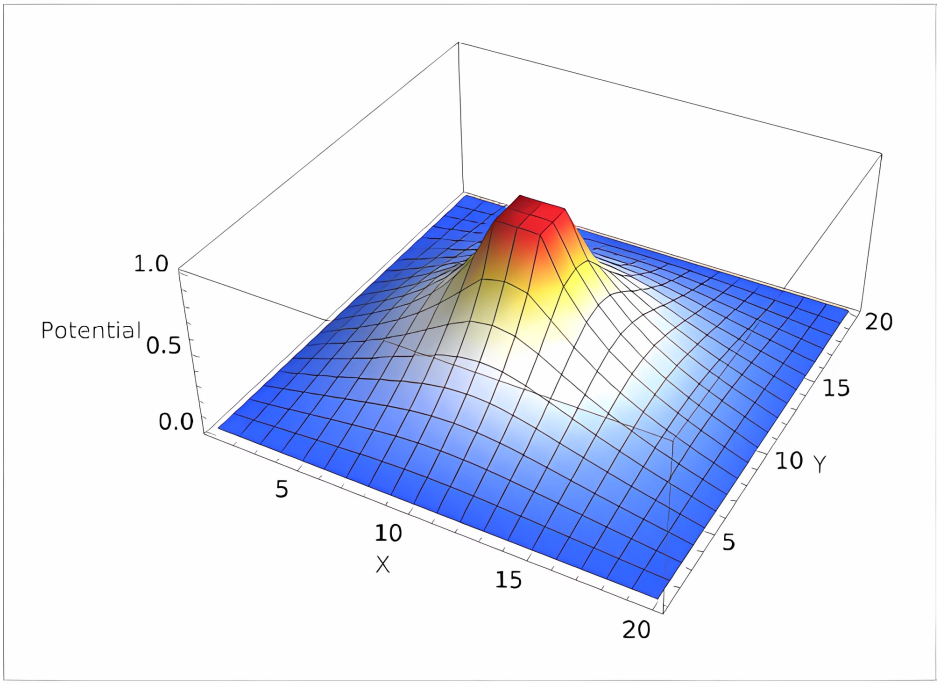

Figure 1.1. The minimizer of the Dirichlet energy with bundary conditions $v \equiv 1$ in B_1 and $v \equiv 0$ in B_{10}^c.

We can now complete the proof of the Mermin–Wagner Theorem for $N = 2$:
Proof of Proposition 1.3.2: Take $\Lambda = B_n$. Let u^* be the minimizer (1.15) with $A = B_\ell$ and $Z = B_n^c$, and set $\Psi = \psi u$. Observe that this choice of Ψ has all the required properties and that $\mathscr{E}(\Psi) = \psi^2 \mathscr{E}(u)$. Using (1.11) and (1.12), we have

$$\begin{aligned} \left| \langle f \rangle_{B_n,\beta}^{\eta} - \langle r_\psi f \rangle_{B_n,\beta}^{\eta} \right| &\leq \|f\|_\infty \sqrt{4C\beta\psi^2 E(u)} \\ &= \|f\|_\infty \sqrt{8C\beta\psi^2 d\,\mathrm{Strength}(i)} \end{aligned}$$

In dimensions $d = 1$ and $d = 2$, recurrence of the symmetric simple random walk implies that $\mathrm{Strength}(i)$ goes to zero as $n \to \infty$ at rates at least (1.9). □

Generalization to N ≥ 3

To prove Theorem 1.3.1 when $N \geq 3$, we reduce the problem to the case $N = 2$. The main observation is that an arbitrary rotation $R \in \mathrm{SO}(N)$ can be obtained as the composition of two dimensional rotations on suitable planes. This means there exists an orthonormal basis, an integer $n \leq N/2$ and n numbers $\psi_i \in (-\pi, \pi]$, such that R can be represented as a block diagonal matrix of the following form:

$$\begin{pmatrix} M(\psi_1) & & & \\ & M(\psi_2) & & \\ & & \ddots & \\ & & & I_{N-2n} \end{pmatrix},$$

where I_{N-2n} is the identity matrix of dimension $N-2n$, and the matrix $M(\psi)$ is given by

$$M(\psi) = \begin{pmatrix} \cos\psi & -\sin\psi \\ \sin\psi & \cos\psi \end{pmatrix}.$$

In particular, R is the composition of n two-dimensional rotations. Therefore, it suffices to prove that any infinite-volume Gibbs measure μ is invariant under such a rotation. In view of the above, we can assume without loss of generality that R has the following block diagonal matrix representation

$$\begin{pmatrix} M(\psi) & 0 \\ 0 & I_{N-2} \end{pmatrix},$$

for some $-\pi < \psi \leq \pi$. Let r be the global rotation associated to R. Since r only affects non-trivially the first two components φ_x^1 and φ_x^2 of the spins φ_x, we introduce the random variables r_x and θ_x, $x \in \mathbb{Z}^d$, such that

$$\varphi_x^1 = r_x \cos\theta_x, \quad \varphi_x^2 = r_x \sin\theta_x.$$

(Notice that $r_x > 0$ almost surely, so that θ_x is almost surely well defined.)

As in the case $N = 2$, we consider an application $\Psi : \mathbb{Z}^d \to (-\pi, \pi]$ such that $\Psi_x = \psi$ for all $x \in B_\ell$, and $\Psi_x = 0$ for all $x \notin B_n$, and let $t_\Psi : \Omega \to \Omega$ be the transformation such that $\theta_x(t_\Psi\omega) = \theta_x(\omega) + \Psi_x$ for all configurations $\omega \in \Omega$.

From this point on, the proof is identical to the $N = 2$ case. The only thing to check is that the relative entropy estimate still works in the same way. But $\varphi_x \cdot \varphi_y$ is actually a function of $\theta_y - \theta_x$, r_x, r_y, and the components φ_x^l, φ_y^l with $l \geq 3$. Since all these quantities except the first one remain constant under the action of t_Ψ, and since the first one becomes $\theta_y - \theta_x + \Psi_y - \Psi_x$, the conclusion follows exactly as before.

1.4 McBryan–Spencer bound

In two dimensions it's possible to improve the bounds of Proposition (1.3.2). McBryan and Spencer established a power law upper bound for the decay of the spin-spin correlation function for these models at low temperatures.

Like in the proof of the Mermin–Wagner theorem, we first prove the result for $N = 2$ (the XY model) and then generalize it to the $N \geq 3$ case.

Theorem 1.4.1. Let $\mu \in \mathcal{G}(2)$ be an infinite volume Gibbs measure associated to the two-dimensional XY model at inverse temperature β. For all $\epsilon > 0$, there exists $\beta_0(\epsilon) < \infty$ such that, for all $\beta > \beta_0(\epsilon)$ and all $x \neq y \in \mathbb{Z}^2$,

$$|\langle \varphi_x \cdot \varphi_y \rangle_\mu| \leq \|y - x\|_2^{-(1-\epsilon)/(2\pi\beta)}.$$

Proof. Without loss of generality, we consider $x = 0$, $y = k$. Similarly to what was done in 1.3.1, we first rely on the DLR property: for all n such that $B_n \ni k$,

$$\langle \varphi_0 \cdot \varphi_k \rangle_\mu = \int \langle \varphi_0 \cdot \varphi_k \rangle_{B_n,\beta}^\eta \mu(d\eta).$$

We will estimate the expectation in the right-hand side, uniformly in the boundary condition η. Observe first that

$$|\langle\varphi_0\cdot\varphi_k\rangle^\eta_{B_n,\beta}| = |\langle\cos(\theta_k-\theta_0)\rangle^\eta_{B_n,\beta}| \le |\langle e^{i(\theta_k-\theta_0)}\rangle^\eta_{B_n,\beta}|,$$

since $|Rez| \le |z|$ for all $z\in\mathbb{C}$. We will write the expectation $\langle\cdot\rangle^\eta_{B_n,\beta}$ using explicit integrals over the angle variables $\theta_x\in(-\pi,\pi]$, $x\in B_n$. As a shorthand, we use the notation

$$\int_{-\pi}^{\pi}\cdots\int_{-\pi}^{\pi}\prod_{x\in B_n}d\theta_x \equiv \int d\theta_{B_n}.$$

Therefore,

$$\langle e^{i(\theta_k-\theta_0)}\rangle^\eta_{B_n,\beta} = \frac{1}{Z^\eta_{B_n,\beta}}\int d\theta_{B_n}\exp\left(i(\theta_k-\theta_0)+\beta\sum_{xy\in E^b_{B_n}}\cos(\theta_y-\theta_x)\right),$$

where $E^b_{B_n} := E_{B_n}\cup\{xy : x\in V_{B_n},\, y\in\mathbb{Z}^2\setminus V_{B_n},\, \|x-y\|_2=1\}$, and we have set $\theta_x=\theta_x(\eta)$ for each $x\notin B_n$. We add an imaginary part to the variables θ_x, $x\in B_n$. Since the integrand is clearly analytic, we can easily deform the integration path associated to the variable θ_x away from the real axis: we shift the integration interval from $[-\pi,\pi]$ to $[-\pi,\pi]+ir_x$, where r_x will be chosen later (also as a function of β and n).

Notice that the periodicity of the integrand guarantees that the contributions coming from the two segments connecting these two intervals cancel each other. We extend the r_x s to a function $r:\mathbb{Z}^2\to\mathbb{R}$, with $r_x=0$ for all $x\notin B_n$. Observe now that

$$|e^{i(\theta_k+ir_k-\theta_0-ir_0)}| = e^{-(r_k-r_0)},$$

$$|e^{\cos(\theta_x+ir_x-\theta_y-ir_y)}| = e^{\cosh(r_x-r_y)\cos(\theta_x-\theta_y)}.$$

We thus have, letting ω_θ denote the spin configuration associated to the angles θ_x,

$$\begin{aligned}
|\langle\varphi_0\cdot\varphi_k\rangle^\eta_{B_n,\beta}| &\le \frac{e^{-(r_k-r_0)}}{Z^\eta_{B_n,\beta}}\int d\theta_{B_n}\exp\left(\beta\sum_{xy\in E^b_{B_n}}\cosh(r_x-r_y)\cos(\theta_x-\theta_y)\right)\\
&= e^{-(r_k-r_0)}\int d\theta_{B_n}\exp\left(\beta\sum_{xy\in E^b_{B_n}}(\cosh(r_x-r_y)-1)\cos(\theta_x-\theta_y)\right)\frac{e^{-\mathcal{H}_{B_n,\beta}(\omega_\theta)}}{Z^\eta_{B_n,\beta}}\\
&= e^{-(r_k-r_0)}\left\langle\exp\left(\beta\sum_{xy\in E^b_{B_n}}(\cosh(r_x-r_y)-1)\cos(\theta_x-\theta_y)\right)\right\rangle^\eta_{B_n,\beta}\\
&\le e^{-(r_k-r_0)}\exp\left(\beta\sum_{xy\in E^b_{B_n}}(\cosh(r_x-r_y)-1)\right).
\end{aligned}$$

In the last inequality, we used the fact that $\cosh(r_x-r_y)\ge 1$ and $\cos(\theta_x-\theta_y)\le 1$. Assume that r can be chosen in such a way that

$$|r_x-r_y|\le C/\beta,\quad \forall xy\in E^b_{B_n}, \tag{1.17}$$

for some constant C. This allows us to replace the cosh term by a simpler quadratic term: given $\epsilon > 0$, we can assume that β_0 is large enough to ensure that $\beta \geq \beta_0$ implies $\cosh(r_x - r_y) - 1 \leq \frac{1}{2}(1+\epsilon)(r_x - r_y)^2$ for all $xy \in E^b_{B_n}$. In particular, we can write

$$\sum_{xy \in E^b_{B_n}} (\cosh(r_x - r_y) - 1) \leq \frac{1}{2}(1+\epsilon) \sum_{xy \in E^b_{B_n}} (r_x - r_y)^2 = (1+\epsilon)\mathscr{E}(r),$$

where $\mathscr{E}(\cdot)$ is the Dirichlet energy functional defined on maps $r : \mathbb{Z}^2 \to \mathbb{R}$ that vanish outside B_n. We thus have

$$|\langle \varphi_0 \cdot \varphi_k \rangle^{\eta}_{B_n,\beta}| \leq \exp\{-\mathscr{D}(r)\},$$

where $\mathscr{D}(\cdot)$ is the functional defined by

$$\mathscr{D}(r) := r_k - r_0 - \beta' \mathscr{E}(r),$$

where we have set $\beta' := (1+\epsilon)\beta$.

As in the proof of the Mermin–Wagner theorem, where we found the minimizer of $\mathscr{E}$, we now look for a maximizer of $\mathscr{D}$.

Lemma 1.4.1. For a fixed $0 \neq k \in B_n$, the functional $\mathscr{D}$ possesses a unique maximizer r^* among the functions r that satisfy $r_x = 0$ for all $x \notin B_n$. That maximizer is the unique such function that satisfies

$$(\Delta r)_x = \frac{1}{2d\beta'}(\mathbb{1}_{\{x=0\}} - \mathbb{1}_{\{x=k\}}), \quad x \in B_n. \tag{1.18}$$

It can be expressed explicitly as

$$r^*_x = \frac{1}{2d\beta'}\left(G_{B_n}(x,k) - G_{B_n}(x,0)\right), \quad x \in B_n,$$

where $G_{B_n}(\cdot,\cdot)$ is the Green function of the symmetric simple random walk in B_n, defined as

$$G_{B_n}(x,y) := \mathbb{E}_x\left[\sum_{k=0}^{\tau_x^+} \mathbb{1}_{\{X_k = y\}}\right]$$

Proof. We start by observing that a critical point r of $\mathscr{D}$ must be such that

$$\frac{d}{ds}\mathscr{D}(r + s\xi)\Big|_{s=0} = 0,$$

for all perturbations $\xi : \mathbb{Z}^d \to \mathbb{R}$ which vanish outside B_n. But, as a straightforward computation shows:

$$\frac{d}{ds}\mathscr{D}(r + s\xi)\Big|_{s=0} = \xi_k\left(1 + 2d\beta'(\Delta r)_k\right) - \xi_0\left(1 - 2d\beta'(\Delta r)_0\right) + 2d\beta' \sum_{x \in B_n \setminus \{0,k\}} \xi_x (\Delta r)_x.$$

Since this sum of three terms must vanish for all ξ, we see that r must satisfy (1.18). The Green function of the random walk is the unique solution to the following discrete Poisson equation:

$$\begin{cases} \Delta f(x) = -\mathbb{1}_{\{x=y\}} & \forall x \in B_n \\ f(x) = 0 & \forall x \in B_n^c \end{cases} \tag{1.19}$$

To see that $G_{B_n}(x,y)$ solves (1.19), i.e. that it's the fundamental solution of the discrete Laplacian operator, we first need to check that it's harmonic for all $x \neq y$, which quickly follows with the same computation used in (1.16); then using again first-step analysis

$$G_{B_n}(0,0) = 1 + \frac{1}{2d} \sum_{x \sim 0} G_{B_n}(x,0)$$

which implies $\Delta G_{B_n}(y,y) = -1$. Zero at the boundary is trivially satisfied since the sum is empty.
To prove that r^* actually maximizes $\mathscr{D}(\cdot)$, let ξ be such that $\xi_i = 0$ outside B_n.

$$\begin{aligned} \mathscr{D}(r^* + \xi) &= \mathscr{D}(r^*) - \beta' \mathscr{E}(\xi) + \xi_k - \xi_0 - \beta'(\nabla \xi, \nabla r^*) \\ &= \mathscr{D}(r^*) - \beta' \mathscr{E}(\xi) + \xi_k - \xi_0 + 2d\beta'(\xi, \Delta r^*) \\ &= \mathscr{D}(r^*) - \beta' \mathscr{E}(\xi). \end{aligned}$$

Since $\mathscr{E}(\xi) \geq 0$, we conclude that $\mathscr{D}(r^* + \xi) \leq \mathscr{D}(r^*)$. □

It follows from the properties of the fundamental solution that there exists a constant C such that $|G_{B_n}(x,v) - G_{B_n}(y,v)| \leq 2C$, uniformly in n, in $v \in B_n$, and for every adjacent vertices x and y [26, Th. B.77]. In particular,

$$|r_x^* - r_y^*| \leq C/\beta,$$

meaning that (1.17) is satisfied. The value of the functional is

$$\mathscr{D}(r^*) = r_k^* - r_0^* - \frac{\beta'}{2}(\nabla r^*, \nabla r^*) = r_k^* - r_0^* - d\beta'(r^*, \Delta r^*) = \frac{r_k^* - r_0^*}{2}$$

We then let $n \to \infty$,

$$\lim_{n \to \infty} \left(G_{B_n}(k,k) - G_{B_n}(k,0) \right) = \lim_{n \to \infty} \left(G_{B_n}(0,0) - G_{B_n}(0,k) \right) = a(k),$$

where $a(k)$ is called the potential kernel of the symmetric simple random walk on $\mathbb{Z}^2$, defined by

$$a(k) := \sum_{m \geq 0} \left(P_0(X_m = 0) - P_k(X_m = 0) \right).$$

Therefore,

$$|\langle \varphi_0 \cdot \varphi_k \rangle_\mu| \leq e^{-a(k)/4\beta'}.$$

The conclusion now follows since, in the case $d = 2$, the potential kernel diverges as

$$a(k) = \frac{2}{\pi} \log \|k\|_2 + O(1)$$

as $\|k\|_2 \to \infty$.

To prove the $N \geq 3$ case, we parameterize the $(N-1)$-sphere by angles $\theta^{(0)}, \theta^{(1)}, \ldots, \theta^{(N-2)}, \phi$ with $|\theta^{(r)}| \leq \pi/2$ for $r = 1, \ldots, N-2$, and $\phi < \pi$, in such a way that only the components φ^1 and φ^2 of a unit spin vector depend on ϕ. We then treat $\langle \varphi_0^1 \varphi_x^1 + \varphi_0^2 \varphi_x^2 \rangle = \frac{2}{N} \langle \varphi_0 \cdot \varphi_x \rangle$ as for the case $N = 2$, translating only the variables ϕ.

□

Chapter 2

Random path representation

The general idea behind expansions of spin models is to rewrite the expected value of multi-point functions as a sum over different combinatorial objects $\mathfrak{X}$. In the case of the Ising model,

$$\langle \sigma_A \rangle = \frac{\sum_{x \in \mathfrak{X}_A} f(x) w(x)}{\sum_{x \in \mathfrak{X}_\emptyset} w(x)}, \qquad \sigma_A := \prod_{x \in A} \sigma_x,$$

where $\mathfrak{X}_\emptyset, \mathfrak{X}_A \subseteq \mathfrak{X}$ and $f, w : \mathfrak{X} \to \mathbb{R}$, with w a non-negative weight function. If $\mathfrak{X}_\emptyset = \mathfrak{X}_A$, then we can view the above sum as the expected value of f with respect to measure w.

In this chapter we will first introduce the random currents expansion for the Ising model, in which the combinatorial objects will be integer valued function of the edge named currents, and use this expansions to prove that in one dimension there is not spontaneous magnetization at any temperature. Then we will use the high-temperature expansion, in which we sum over subgraphs, to prove the exponential decay of correlations at high temperature. Finally we introduce the expansion that names this chapter, the random path model. As the name suggests, the combinatorial objects are colored paths (open trails) or loops (circuits). We then prove, exploiting the connection between loop connectivity and spin-spin correlation, that the probability that two vertices are connected by a loop decreases at least algebraically with their distance.

2.1 Random current representation of the Ising model

In this section we rewrite the expected value of multi-point functions for the Ising model as a sum over non-negative integer valued functions over the edges, named *currents*. Using this representation we immediately deduce the first Griffiths inequality, and easily compute the spontaneous magnetization in $d = 1$.

Definition 2.1.1. A *current* on a finite simple graph $G = (V, E)$ is a function

$$\mathbf{n} : E \to \mathbb{N}$$

The *sources* of $\mathbf{n}$ are the subset of vertices $\partial\mathbf{n} \subseteq V$ such that

$$\partial\mathbf{n} := \left\{ x \in V \, : \, \sum_{y \sim x} n_{xy} \in 2\mathbb{N} + 1 \right\}$$

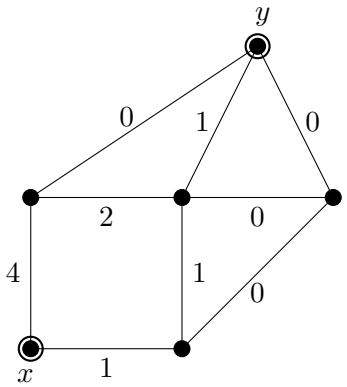

Figure 2.1. A current with sources $\partial\mathbf{n} = \{x, y\}$.

Theorem 2.1.1. Consider the Ising model with free boundary conditions on a simple graph $G = (V, E)$, then given $A \subseteq V$ the expected value of the multi-point function is

$$\langle \sigma_A \rangle = \frac{\sum_{\partial\mathbf{n}=A} w(\mathbf{n})}{\sum_{\partial\mathbf{n}=\emptyset} w(\mathbf{n})}, \qquad w(\mathbf{n}) := \prod_{e\in E} \frac{J_e{}^{n_e}}{n_e!}$$

Proof. The main idea is to Taylor expand each weight $e^{J_{xy}\sigma_x\sigma_y}$, then expand the product and rearrange terms (each sum is absolutely convergent).

$$e^{-\mathcal{H}(\omega)} = \prod_{xy\in E} e^{J_{xy}\sigma_x\sigma_y} = \prod_{xy\in E}\sum_{n\geq 0} \frac{(J_{xy}\sigma_x\sigma_y)^n}{n!}$$

$$= \sum_{\mathbf{n}\in\mathbb{N}^E} \prod_{xy\in E} \frac{(J_{xy}\sigma_x\sigma_y)^{n_{xy}}}{n_{xy}!} = \sum_{\mathbf{n}\in\mathbb{N}^E} \prod_{e\in E} \frac{J_e^{n_e}}{n_e!} \prod_{xy\in E} (\sigma_x\sigma_y)^{n_{xy}}$$

Each factor in the second product σ_x appears raised to the power $\sum_{e\ni x} n_e$, hence it contributes to the product in a non trivial way only if it is raised to an odd power, that is $x \in \partial\mathbf{n}$.

Using this expression and permuting the sum over states:

$$Z[\sigma_A] = \sum_{\omega\in\Omega} \sigma_A e^{-\mathcal{H}(\omega)} = \sum_{\mathbf{n}\in\mathbb{N}^E} \prod_{e\in E} \frac{J_e^{n_e}}{n_e!} \sum_{\omega\in\Omega} \sigma_A\sigma_{\partial\mathbf{n}}$$

Using the fact that

$$\sum_{\omega\in\Omega} \sigma_A\sigma_B = \begin{cases} |\Omega| & \text{if } A = B \\ 0 & \text{otherwise} \end{cases}$$

and that $\langle\sigma_A\rangle = \frac{Z[\sigma_A]}{Z[1]}$, we get our result. □

Since each term in the numerator is non-negative, and positive in the denumeratorm, we deduce that the expected value of multi-point functions is always non negative.

Corollary 2.1.1. (First GKS inequality) For every $A \subseteq V$ we have

$$\langle \sigma_A \rangle \geq 0$$

We will now use this representation to compute the spontaneuous magnetization for the one dimensional Ising model with +1 boundary conditions:

$$m(\beta) = \lim_{n\to\infty} \langle\sigma_0\rangle^+_{\Lambda_n}$$

with $\Lambda_n = \{-n, \dots, n\}$. Consider the graph G_n obtained by identifying the two vertices $-n$ and $+n$ into a new vertex called g. Using spin flip symmetry it's easy to show that

$$\langle\sigma_A \mid \sigma_g = +1\rangle = 2\langle\sigma_A \mathbb{1}_{\sigma_g=+1}\rangle = \langle\sigma_A\sigma_g\rangle + \langle\sigma_A\rangle$$

Then considering a single spin, the second term is zero again by spin flip symmetry, and we can write

$$\langle\sigma_0\rangle^+_{\Lambda_n} = \langle\sigma_0 \mid \sigma_g = +1\rangle_{G_n} = \langle\sigma_0\sigma_g\rangle_{G_n}$$

We can interpret the expression of the weight $w(\mathbf{n})$ on currents as independent poisson processes with parameter J_e, and introduce a probability measure on currents:

$$P(\mathbf{n}) := \frac{w(\mathbf{n})}{\sum_{\mathbf{m}} w(\mathbf{m})} \tag{2.1}$$

From the previous theorem we know

$$\langle\sigma_0\sigma_g\rangle_{G_n} = \frac{P(\partial\mathbf{n} = \{0, g\})}{P(\partial\mathbf{n} = \emptyset)}$$

The probability of a Poisson random variable of being even is

$$\sum_{n\in 2\mathbb{N}} e^{-\lambda}\frac{\lambda^n}{n!} = e^{-\lambda}\cosh\lambda$$

and odd with probability $e^{-\lambda}\sinh\lambda$. A random current is sourceless if all the values n_e have the same parity. Since they are independent poisson random variables, this event has probability

$$P(\partial\mathbf{n} = \emptyset) = \prod_{e\in E} e^{-2J_e}(\sinh^2 J_e + \cosh^2 J_e)$$

Similarly, 0 and g are the sources of $\mathbf{n}$ if and only if the edges on opposite sides have different parity

$$P(\partial\mathbf{n} = \{0, g\}) = 2\prod_{e\in E_1} e^{-J_e}\cosh J_e \prod_{e\in E_2} e^{-J_e}\sinh J_e$$

Finally we obtain

$$\langle\sigma_0\rangle^+ = \lim_{n\to\infty} \frac{2\prod_{e\in E_1} e^{-J_e}\cosh J_e \prod_{e\in E_2} e^{-J_e}\sinh J_e}{\prod_{e\in E} e^{-2J_e}(\sinh^2 J_e + \cosh^2 J_e)}$$

If we set $J_e = \beta$ for all $e \in E$, this expression simplyfies to

$$\frac{2\sinh^n\beta\cosh^n\beta}{\sinh^{2n}\beta + \cosh^{2n}\beta} = \frac{2\tanh^n\beta}{\tanh^{2n}\beta + 1} \le 2\tanh^n\beta$$

which tends to zero as n goes to infinity for every finite inverse temperature β, hence $\beta^c_{mag} = \infty$ in dimension 1.

2.2 Exponential decay of correlations at high temperature

We show that at (finite) high enough temperature we have exponential decay of correlations in every dimension. To do this we employ the *high-temperature expansion*, rewriting the partition function as a sum over subgraphs.

Start by adding and subtracting β in the arguments of the exponential terms of the partition function:

$$Z^{spin}_{G,N,\beta} = \int_{\Omega_G} \prod_{\{x,y\}\in E} e^{\beta\varphi_x\cdot\varphi_y}\, d\omega = e^{-\beta|E|}\int_{\Omega_G} \prod_{\{x,y\}\in E} e^{\beta(\varphi_x\cdot\varphi_y+1)}\, d\omega$$

now define $f_\beta(\varphi_x,\varphi_y) := e^{\beta(\varphi_x\cdot\varphi_y+1)} - 1$

$$e^{-\beta|E|}\int_{\Omega_G} \prod_{\{x,y\}\in E} (f_\beta(\varphi_x,\varphi_y)+1)\, d\omega$$

$$= e^{-\beta|E|}\sum_{F\subseteq E}\int_{\Omega_G} \prod_{\{x,y\}\in F} f_\beta(\varphi_x,\varphi_y)\, d\omega$$

where we have used the fact that

$$\prod_{e\in E}(1+x_e) = \sum_{F\subseteq E}\prod_{e\in F} x_e.$$

Thus we have

$$Z^{spin}_{G,N,\beta} = e^{-\beta|E|}\sum_{F\subseteq E} Z(F)$$

with

$$Z(F) := \int_{\Omega_G} \prod_{\{x,y\}\in F} f_\beta(\varphi_x,\varphi_y)\, d\omega \tag{2.2}$$

since f_β is non-negative, me may interpret as a probability measure on subgraphs of G, where each subgraph (V,F) has probabitlity proportional to $Z(F)$. Furthermore, for a fixed subgraph, we may intepret as a probability on spin configurations ω, with density proportional to

$$Z(F,\omega) := \prod_{\{x,y\}\in F} f_\beta(\varphi_x,\varphi_y)$$

Theorem 2.2.1. Consider the spin O(N) model on a finite simple graph G with maximum degree Δ. For every $N \geq 1$, this model exhibits exponential decay of correlations at high temperatures. Precisely, there exists $\beta_0(\Delta,N)$ such that for all $\beta < \beta_0(\Delta,N)$, the correlation between any two vertices $x,y\in V$ satisfies:

$$\langle\varphi_x\cdot\varphi_y\rangle \leq C_{\Delta,N}e^{-c_{\Delta,N,\beta}d_G(x,y)},$$

where $C_{\Delta,N}$ and $c_{\Delta,N,\beta}$ are positive constants dependent on Δ, N, and β. Furthermore, for one-dimensional models ($\Delta = 2$), the exponential decay of correlations persists for all finite values of β.

Proof. The key observation is that, conditioned on a subgraph F, spins φ_x and φ_y are independent if x and y are not connected in F, $\langle \varphi_x \cdot \varphi_y \mid F \rangle = 0$, then

$$\langle \varphi_x \cdot \varphi_y \rangle = \sum_{\substack{F \subseteq E \\ x \leftrightarrow y}} \langle \varphi_x \cdot \varphi_y \mid F \rangle P(F) \leq P(x \leftrightarrow y \text{ in } (V, F))$$

where F is chosen according to 2.2. To establish the decay of correlations it suffices to show that long connections are unlikely. First fix a subset F and an edge $e \in F$.

$$P(e \in F \mid F \setminus \{e\} = F_0) = \frac{Z(F_0 \cup \{e\})}{Z(F_0 \cup \{e\}) + Z(F_0)}$$

denoting $e = \{u, v\}$ and using the fact that $f_\beta \leq e^{2\beta} - 1$,

$$\frac{Z(F_0 \cup \{e\})}{Z(F_0)} = \frac{\int_{\Omega_G} Z(F_0 \cup \{e\}, \omega) d\omega}{\int_{\Omega_G} Z(F_0, \sigma) d\omega} = \frac{\int_{\Omega_G} Z(F_0, \omega) f_\beta(\varphi_u, \varphi_v) d\omega}{\int_{\Omega_G} Z(F_0, \omega) d\omega} \leq e^{2\beta} - 1$$

From this follows setting $F_0 = \emptyset$ that $P(e_1 \in F) \leq 1 - e^{-2\beta}$, and

$$P(e_2 \in F, e_1 \in F) = P(e_2 \in F \mid e_1 \in F) P(e_1 \in F) \leq (1 - e^{-2\beta})^2$$

so that the probability that F contains any subgraph consisting of K edges $e_1, \ldots, e_k \in E$ is exponentially small in K:

$$P(e_1 \in F, \ldots, e_k \in F) \leq (1 - e^{-2\beta})^k$$

Let Δ be the maximum degree of graph G (in the case of square lattices $\Delta = 2d$). The event that x and y are connected in (V, F) implies the existence of a simple path in F of some length $k \geq d_G(x, y)$. Since the number of simple paths is at most $\Delta(\Delta - 1)^{k-1} \leq 2(\Delta - 1)^k$, we obtain

$$P(x \leftrightarrow y \text{ in } F) \leq \sum_{k \geq d_G(x,y)} 2(\Delta - 1)^k (1 - e^{-2\beta})^k \leq C_{\Delta,\beta} \left((\Delta - 1)(1 - e^{-2\beta}) \right)^{d_G(x,y)}$$

provided that $(\Delta - 1)(1 - e^{-2\beta}) < 1$. Thus, we have established that

$$|\langle \varphi_x \cdot \varphi_y \rangle| \leq C_{d,\beta} e^{-c_{\Delta,\beta} d_G(x,y)} \qquad \text{when } \beta < \frac{1}{2} \log \frac{\Delta - 1}{\Delta - 2}$$

This proves exponential decay of correlations for every lattice with $d \geq 2$ with β small enough, and for all finite β in the case $d = 1$. □

2.3 Random path representation

In this section we try to follow the route of the first section but for continuous spins, that is $N \geq 2$. The representation we will obtain is unfortunately less straight forward, and involves a more complicated objects namely *paths* with *colors* and *pairings*.

Consider a simple finite graph $\mathcal{G} = (\mathcal{V}, \mathcal{E})$. Let $N \geq 1$ be the number of *colors*. A configuration of the Random Path Model (RPM) can be views as a collection of

colored paths, where each path is identified by a colouring, a collection of links, and by pairings.

As in the case of the random currents expansion, we introduce an integer valued edge function, or equivalently the collection

$$m = (m_e)_{e\in\mathcal{E}}, \quad m_e \in \mathbb{N}$$

and denote the set of such collection on a graph $\mathcal{G}$ by $\mathcal{M}_\mathcal{G}$.

A *colouring* for a given link configuration $m \in \mathcal{M}_\mathcal{G}$, is a function which assigns a color to each link, that is $c = (c_e)_{e\in\mathcal{E}}$ with $c_e : \{1, \dots, m_e\} \to [N]$. We call links of color $i \in [N]$ i-links. We denote the set of all possible colorings of a given link configuration by $\mathcal{C}_\mathcal{G}(m)$. For a given edge $e \in \mathcal{E}$, we denote by m_e^i as the number of i-links on e.

Given a link configuration $m \in \mathcal{M}_\mathcal{G}$, and on of its colouring $c \in \mathcal{C}_\mathcal{G}(m)$, a *pairing* $\pi = (\pi_x)_{x\in\mathcal{V}}$, where π_x is a partition of the links incident to vertex x such that each has set of the partition contains only links of the same color and has cardinality of one or two. We denote by $\mathcal{P}_\mathcal{G}(m, c)$ the set of all possible pairings for m and c.

A configuration of the RPM model is a tuple $w = (m, c, \pi)$ such that $m \in \mathcal{M}_\mathcal{G}$, $c \in \mathcal{C}_\mathcal{G}(m)$ and $\pi \in \mathcal{P}_\mathcal{G}(m, c)$, and denote the set of all configurations by $\mathcal{W}_\mathcal{G}$. By choosing a starting link and proceeding by following paired links, we can easily see that a configuration of the RPM can be viewed as a collection of colored paths. We refer to paths of color $i \in [N]$ as i-paths, or i-loops if they are closed.

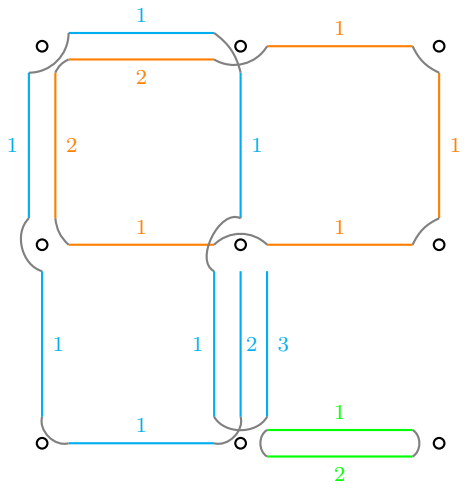

Figure 2.2. A configuration $w \in (m, c, \pi) \in \mathcal{W}_G$, where G corresponds to the graph $\{1, 2, 3\}^2$. On every edge e, the links are ordered and receive a label from 1 to m_e. The numbers $1, 2, \dots$ are used for the identification of the links, and the color of each edge represents the color assigned by c, here $N = 3$. Pairings are represented in gray. There are only two unpaired links, both incident at the center vertex.

If in a vertex we have an unpaired link, this means it's one of the endpoints of an open path. On the other end, paired links are in a path that crosses that vertex. If we imagine these paths as trails of a random walk, then the number of visits to a given vertex $x \in \mathcal{V}$, which we refer to as *local time*, is the number of paired links incident to x divided by two, plus the number of unpaired links: unpaired end-points

of links touching x and pairs of paired links touching x both contribute $+1$ to the local time. Given a color i, let $u_x^i(w)$ and $v_x^i(w)$ be the number of unpaired and paired i-links at vertex x, respectively. Then the local time of color i $n_x^i(w)$ and the total local time $n_x(w)$ are defined as

$$n_x^i(w) := u_x^i(w) + \frac{1}{2}v_x^i(w) \qquad n_x(w) := \sum_{i=1}^{N} n_x^i(w)$$

Since we want to obtain a representation for the Spin O(N) model with possibly an external magnetic field, we introduce a ghost vertex g, and work with the graph $G = (V, E)$ defined as

$$V = \mathcal{V} \cup \{g\}, \qquad E = \mathcal{E} \cup \{\{x, g\} \,:\, x \in \mathcal{V}\}$$

We now define a subset of the possible configuration, which will reflect our goal of computing the spin-spin correlation along the e_1 direction, with an external magnetic field pointing in the e_N direction. We will see that the sum in the expansion will only involve configurations with closed loops of color $1, 2, \ldots, N-1$, open paths of color N with both endpoints at the ghost vertex g, and open paths of color 1.

Definition 2.3.1. We let $\mathcal{W}'_G$ be the set of configurations $w \in \mathcal{W}_G$ such that $v_g^N(w) = n_g^1(w) = \cdots = n_g^{N-1}(w) = 0$ and $u_2^x(w) = \cdots = u_x^N(w) = 0$ for every $x \in \mathcal{V}$. Given $N \in \mathbb{N} > 0$, $\beta \in \mathbb{R} \geq 0$, $h \in \mathbb{R}$, we define the non-negative measure $\mu_{G,N,\beta,h}$ on $\mathcal{W}'_G$ as follows, for any $w = (m, c, \pi) \in \mathcal{W}'_G$,

$$\mu_{G,N,\beta,h}(w) = \prod_{e\in\mathcal{E}} \frac{\beta^{m_e}}{m_e!} \prod_{x\in\mathcal{V}} \frac{h^{m_{\{x,g\}}}}{m_{\{x,g\}}!} \prod_{x\in\mathcal{V}} U_x(w), \tag{2.3}$$

where $U_x(w) = U(n_x(w))$, with

$$\forall r \in \mathbb{N}, \quad U(r) := \frac{\Gamma(\frac{N}{2})}{2^r \Gamma(r + \frac{N}{2})}.$$

This measure is a special case of a class of measures introduced in [28], in which different weight functions U are considered, together with long range interactions through a potential function.

The expected value with respect to this measure will be denoted by $\mathbb{E}[\cdot]$.

Definition 2.3.2. For $A \subset V$, define $\mathcal{S}(A)$ to be the set of configurations $w \in W'_G$ such that $u_z^1(w) = 1$ for every $z \in A$ and $u_z^1(w) = 0$ for every $z \in V \setminus A$. We define $Z_{G,N,\beta,h}(A) = \mu_{G,N,\beta,h}(S(A))$ and $Z_{G,N,\beta,h} = \mu_{G,N,\beta,h}(S(\emptyset))$. Finally, we define the point-to-point correlation functions by,

$$\mathbb{G}_{G,N,\beta,h}(A) := \frac{Z_{G,N,\beta,h}(A)}{Z_{G,N,\beta,h}(\emptyset)}.$$

We call the cases where $|A| = 2$ two-point functions. When $A = \{x, y\}$ for $x \neq y$ we write $Z_{G,N,\beta,h}(x, y)$ and $\mathbb{G}_{G,N,\beta}(x, y)$ for $Z_{G,N,\beta,h}(A)$ and $\mathbb{G}_{G,N,\beta}(A)$ respectively. We also write $\mathcal{S}_G$ for $\mathcal{S}(\emptyset)$.

The next proposition connects this ratio of partition functions to the correlation function in spin models.

Proposition 2.3.1. Let $G = (V, E)$ be a finite simple graph. Let $N \in \mathbb{N}_0$, $\beta \geq 0$ and $h \in \mathbb{R}$. We have that,

$$\mathbb{G}_{G,N,\beta,h}(A) = \left\langle \prod_{x \in A} \varphi_x^1 \right\rangle_{G,N,\beta,h}^{\text{spin}}.$$

Proof. To begin, for $A \subseteq V$ we define

$$Z_{G,N,\beta,h}^{\text{spin}}(A) := Z_{G,N,\beta,h}^{\text{spin}} \left\langle \prod_{x \in A} \varphi_x^1 \right\rangle_{G,N,\beta,h}^{\text{spin}} = \int_\Omega d\omega \left(\prod_{x \in A} \varphi_x^1 \right) e^{-\beta \mathcal{H}_{G,N,\beta,h}(\varphi)}.$$

Before starting to expand the exponential terms, we introduce a clever notation to avoid having to distinguish constantly between cases:

$$J_{xy}^i = \begin{cases} \beta & \text{if } xy \in E \\ h & \text{if } x = g \text{ or } x = y, \text{ and } i = N \\ 0 & \text{otherwise} \end{cases}$$

We now write the exponential term as a product,

$$\exp\left(\sum_{\{x,y\} \in E} \sum_{i=1}^{N} J_{xy}^i \varphi_x^i \varphi_y^i \right) = \prod_{\{x,y\} \in \mathcal{E}} \prod_{i=1}^{N} e^{J_{xy}^i a \varphi_x^i \varphi_y^i}.$$

and Taylor expand each exponential just like in the random currents representation

$$e^{\beta \varphi_x^i \varphi_y^i} = \sum_{m_{\{x,y\}}^i \geq 0} \frac{(J_{xy}^i)^{m_{\{x,y\}}^i} (\varphi_x^i \varphi_y^i)^{m_{\{x,y\}}^i}}{m_{\{x,y\}}^i!}.$$

Using this in the definition of $Z_{G,N,\beta,h}^{\text{spin}}(A)$ we get

$$Z_{G,N,\beta,h}^{\text{spin}}(A) = \prod_{\{x,y\} \in E} \prod_{i=1}^{N} \sum_{m_{\{x,y\}}^i \geq 0} \frac{(J_{xy}^i)^{m_{\{x,y\}}^i}}{m_{\{x,y\}}^i!} \int d\varphi \left(\prod_{x \in A} \varphi_x^1 \right) (\varphi_x^i \varphi_y^i)^{m_{\{x,y\}}^i}$$

since the series for the exponential converges absolutely, we can exchange the sum with the integral

$$= \sum_m \prod_{\{x,y\} \in E} \prod_{i=1}^{N} \frac{(J_{xy}^i)^{m_{\{x,y\}}^i}}{m_{\{x,y\}}^i!} \int d\varphi \left(\prod_{x \in A} \varphi_x^1 \right) (\varphi_x^i \varphi_y^i)^{m_{\{x,y\}}^i}$$

Now we claim that the integral is non-zero only if the exponents of each φ_x^i is even. Then we can restrict the sum over edge functions m that for each color i make the

exponent odd if $x \in A$ and $i = 1$, due to the factor $\prod_{x\in A} \varphi_x^1$, and even for all other cases.

By exchanging the product over edges with the integral, we see that each φ_x^i is raised to the power $q_x^i(m) := \sum_{e\ni x} m_e^i$ if $x \in V \setminus A$, and to the power $q_x^i(m) + 1$ if $x \in A$ and $i = 1$.

By remembering that $J_{xg}^i = 0$ if $i \neq N$, we see that for every component different from N we can sum over configurations which are nonzero only in the edges of the original graph $\mathcal{G}$.

Given $B \subseteq V$ we define sets

$$\widetilde{\mathcal{M}}_G(B) = \left\{ m \in \mathcal{M}_G : \forall x \in B \quad m_e \in 2\mathbb{N}+1, \quad \forall x \in V\setminus B \sum_{e\in E: x\in e} m_e \in 2\mathbb{N} \right\}$$

$$\mathcal{M}_{\mathcal{G}}(B) = \widetilde{\mathcal{M}}_G(B) \cap \left\{ m \in \mathcal{M}_G \,:\, \sum_{x\in\mathcal{V}} m_{xg} = 0 \right\}$$

Using Fubini to combine the sums we have

$$= \sum_{\substack{m^1\in\mathcal{M}_{\mathcal{G}}(A)\\ m^2,\dots,m^{N-1}\in\mathcal{M}_{\mathcal{G}}(\emptyset)\\ m^N\in\widetilde{\mathcal{M}}_G(\emptyset)}} \prod_{e\in E}\prod_{i=1}^N \frac{(J_e^i)^{m_e^i}}{m_e^i!} \int_\Omega d\varphi \left(\prod_{x\in A} (\varphi_x^i)^{q_x^i+1} (\varphi_x^2)^{q_x^2} \cdots (\varphi_x^N)^{q_x^N} \right)$$
$$\times \left(\prod_{x\in V\setminus A} (\varphi_x^i)^{q_x^i} (\varphi_x^2)^{q_x^2} \dots (\varphi_x^N)^{q_x^N} \right)$$

Now we use the following identity

$$\int_{S^{N-1}} (\varphi^1)^{n_1} \dots (\varphi^N)^{n_N} d\varphi = \begin{cases} \frac{\Gamma\left(\frac{N}{2}\right) \prod_{i=1}^N (n_i-1)!!}{2^{n/2}\Gamma\left(\frac{n+N}{2}\right)} & \text{if } n_i \in 2\mathbb{N} \text{ for } i \in [N], \\ 0 & \text{otherwise.} \end{cases}$$

with $n = \sum_{i=1}^N n_i$.

We now sum over uncolored link configuration, then distribute over all colors

$$Z^{\text{spin}}_{G,N,\beta,h}(A) = \sum_{m\in\widetilde{\mathcal{M}}_G(A)} \left(\prod_{e\in E} \frac{1}{m_e!} \right) \sum_{\substack{m^1\in\widetilde{\mathcal{M}}_G(A), m^N\in\widetilde{\mathcal{M}}_G(\emptyset)\\ m^2,\dots,m^{N-1}\in\mathcal{M}_{\mathcal{G}}(\emptyset)\\ \sum_{i=1}^N m^i = m}} \left(\prod_{e\in E} \frac{m_e!}{m_e^1! \dots m_e^N!} \right) \left(\prod_{i=1}^N (J_e^i)^{m_e^i} \right)$$
$$\left(\prod_{x\in A} \frac{\Gamma\left(\frac{N}{2}\right)}{2^{(q_x+1)/2}\Gamma\left(\frac{q_x+1+N}{2}\right)} (q_x^1!!) \prod_{i=2}^N (q_x^i-1)!! \right) \left(\prod_{x\in V\setminus A} \frac{\Gamma\left(\frac{N}{2}\right)}{2^{q_x/2}\Gamma\left(\frac{q_x+N}{2}\right)} \prod_{i=1}^N (q_x^i-1)!! \right). \tag{2.4}$$

We can give a nice combinatorial interpretation to the double factorials in terms of pairings:

$$\prod_{x\in A} q_x^1!! \prod_{i=2}^{N}(q_x^i-1)!! \qquad \prod_{x\in V\setminus A}\prod_{i=1}^{N}(q_x^i-1)!!$$

$(q-1)!!$ is the number of pefect matching in a graph with q vertices if q is even, and is the number of perfect matching leaving one vertex left out if q is odd. We can match, or pair, a link of a given color with another link of the same color incident at the same vertex.

Then the terms that appear in our partition function can be interpreted as the number of such pairing configurations. By defining $n_x(w) := \frac{q_x+1}{2}$ if $x \in A$ and $n_x(w) = \frac{q_x}{2}$ otherwise, and doing the same expansion for $Z^{\text{spin}}_{G,N,\beta,h}(\emptyset)$ we get our result.

□

Remark 2.3.1. The equivalence remains valid in the absence of an external magnetic field ($h = 0$). In this simpler case, which we refer to as *zero-field*, the introduction of a ghost vertex is unnecessary, and the relevant configurations consists of closed loops of any color, while allowing an open path of color 1.

Corollary 2.3.1 (Griffiths first inequality)**.** The equivalence also shows that $\langle\varphi_x^1\varphi_y^1\rangle \geq 0$, since each term in the expansion is positive (h is always raised to an even power).

This expansion was used in [1] to prove that with a non-zero external magnetic field, transverse correlations decay exponentially to zero at all inverse temperatures. Here we state the result without proof, which uses a clever color-switch lemma that relates the ratio of partition functions to the expected number of N-walks with their two last steps on the edges $\{x, g\}$ and $\{y, g\}$, and then shows that this value is exponentially small with respect to $d_G(x, y)$.

Theorem 2.3.1 (Lees–Taggi)**.** Let G be an infinite simple graph with bounded degree. For any $h \neq 0$, $\beta \geq 0$ and $N \in \mathbb{N}_{\geq 2}$ there are positive constants $c_0 = c_0(G, \beta, h, N)$ and $C_0 = C_0(G, \beta, h, N)$ such that the following holds. Let $(G_L)_{L\in\mathbb{N}}$, with $G_L = (V_L, E_L) \subset G$, be an arbitrary sequence of finite graphs. Then, for any $L \in \mathbb{N}$ and any $x, y \in V_L$,

$$\langle\varphi_x^1\varphi_y^1\rangle_{G_L,N,\beta,h} \leq C_0 e^{-c_0 d_G(x,y)},$$

where $d_G(x, y)$ denotes the graph distance between x and y in G. Moreover, the choice of c_0 can be made so that, $c_0 = O(h^2)$ in the limit as $h \to 0$.

2.4 Spin-Spin correlation and loop connectivity

Unfortunately, it's not clear how to rewrite the partition function ratio as the probability of some event (this can be done for the random current expansion of the Ising model using the Switch Lemma [29]). However, if we attempt to compute the following mixed spin-spin correlation

$$\langle\varphi_x^1\varphi_y^1\varphi_x^2\varphi_y^2\rangle,$$

which involves different components, there is a simple transformation of the configuration that allows us to relate this correlation with the probability of observing a loop connecting x and y.

We consider the zero-field measure, where the introduction of a ghost vertex is unnecessary (See Remark 2.3.1). In this case, the set $\mathcal{S}_G = \mathcal{S}(\emptyset)$ represents configurations consisting only of closed loops. We define $\mathcal{S}^{1,2}(\{x,y\})$ as the set of configurations featuring a unique open 1-path P_1, and a unique open 2-path P_2, both connecting vertices x and y. Then, it is evident that an equivalence similar to (2.3.1) holds:

$$\langle \varphi_x^1 \varphi_y^1 \varphi_x^2 \varphi_y^2 \rangle = \frac{1}{Z_{G,N,\beta}} \sum_{w \in \mathcal{S}^{1,2}(\{x,y\})} \mu(w)$$

We still have the problem that in the numerator we sum over a set of configurations not contained in the sum of the partition function. A clever trick to solve this issue is presented in [28, Lemma 5.4]: change the color of one of the two paths joining x and y, for instance, converting the 2-path to a 1-path. We then obtain a state in which only closed loops are present, and x and y joined by a loop of color 1. Denote this set of states by $\mathcal{S}^1(\{x,y\})$, a subset of $\mathcal{S}_G$. This transformation preserves the number of links and the local times, except at vertices x and y, where they decrease by one.

We let $\zeta_1(w)$ denote the set of 1-cycles in the configuration w, and for any cycle $\chi \in \zeta_1(w)$ and vertex $x \in V$, we define $n_x^{(\chi)}$ as the number of times the cycle χ visits vertex x. This quantity is calculated as follows:

$$n_x^{(\chi)} := \frac{1}{2} \sum_{y \sim x} \sum_{p=1}^{m_{\{x,y\}}} \mathbb{1}_{(\{x,y\},p) \in \chi},$$

In other words, $n_x^{(\chi)}$ is the number of links contained in χ touching x divided by two.

Proposition 2.4.1. For any $N \geq 2$, $m \in \mathbb{N}$, $\beta \in \geq 0$ and any $x \neq y \in \Lambda$, it holds that,

$$cP(x \leftrightarrow y)^{1+\frac{1}{2(m-1)}} \leq \langle \varphi_x^1 \varphi_y^1 \varphi_x^2 \varphi_y^2 \rangle \leq \frac{1}{2N} P(x \leftrightarrow y)$$

where $c = c(d, \beta, N, m) > 0$ and $\{x \leftrightarrow y\}$ is the event that vertices x and y are connected by a loop.

Proof. We define a map $F : \mathcal{S}^{1,2}(\{x,y\}) \to \mathcal{S}^1(\{x,y\})$ which acts by changing the 2-path P_2 to a 1-path and pairs the endpoints of the 1-paths joining x and y, introducing a 1-loop. This map is surjective but not injective; for any $w' \in \mathcal{S}^1(\{x,y\})$, $F^{-1}(w')$ consists of configurations in $\mathcal{S}^{1,2}(\{x,y\})$ obtained by choosing a cycle that joins x and y, changing the color of one of its paths and unpairing the endpoints. Hence

$$|\{w \in \mathcal{S}^1(\{x,y\}) \,:\, F(w) = w'\}| = 2 \sum_{\chi \in \zeta^1(w)} n_x^{(\chi)} n_y^{(\chi)}.$$

This transformation preserves the number of links and local times, except at x and y, where they decrease by one:

$$n_x(w') = n_x(w) - 1, \qquad n_y(w') = n_y(w) - 1.$$

Consequently,

$$\mu(w) = \frac{1}{4}\mu(w')\left(\frac{N}{2} + n_x(w')\right)^{-1}\left(\frac{N}{2} + n_y(w')\right)^{-1} = \frac{1}{4}\mu(w')\frac{1}{\tilde{n}_x(w')\tilde{n}_y(w')}$$

Where we have defined $\tilde{n}_x(w) := N/2 + n_x(w)$ for convenience. Then

$$\begin{aligned}
\langle \varphi_x^1\varphi_y^1\varphi_x^2\varphi_y^2\rangle &= \frac{1}{Z_{G,N,\beta,h}}\sum_{w\in\mathcal{S}^{1,2}(\{x,y\})}\mu(m)\\
&= \frac{1}{4Z_{G,N,\beta,h}}\sum_{w\in\mathcal{S}^{1,2}(\{x,y\})}\mu(F(w))\frac{1}{\tilde{n}_x(w')\tilde{n}_y(w')}\\
&= \frac{1}{2Z_{G,N,\beta,h}}\sum_{w'\in\mathcal{S}^{1}(\{x,y\})}\mu(w')\sum_{\chi\in\zeta^1(w')} n_x^{(\chi)}n_y^{(\chi)}\frac{1}{\tilde{n}_x(w')\tilde{n}_y(w')}\\
&= \frac{1}{2}\mathbb{E}\left[\mathbb{1}_{\{x\overset{1}{\leftrightarrow}y\}}\sum_{\chi\in\zeta^1(w')} n_x^{(\chi)}n_y^{(\chi)}\frac{1}{\tilde{n}_x(w')\tilde{n}_y(w')}\right] \qquad (2.5)\\
&\leq \frac{1}{2}P(x\overset{1}{\leftrightarrow}y) = \frac{1}{2N}P(x\leftrightarrow y) \qquad (2.6)
\end{aligned}$$

since, by observing that if $w\in\mathcal{S}_G$, $n_x(w) = \sum_{i=1}^N\sum_{\chi\in\zeta^i(w)} n_x^{(\chi)}$, we can conclude

$$\sum_{\chi\in\zeta^1(w')} n_x^{(\chi)}n_y^{(\chi)} \leq \tilde{n}_x(w')\tilde{n}_y(w').$$

In the last equality (2.6) we used the fact that in the zero-field case there is symmetry among colors.

To obtain the lower bound, we iteratively apply the Cauchy-Schwarz inequality m times:

$$\begin{aligned}
P(x\leftrightarrow y) &= \mathbb{E}\left[\mathbb{1}_{\{x\leftrightarrow y\}}\frac{1}{\sqrt{\tilde{n}_x(w)\tilde{n}_y(w)}}\sqrt{\tilde{n}_x(w)\tilde{n}_y(w)}\right]\\
&\leq \mathbb{E}\left[\mathbb{1}_{\{x\leftrightarrow y\}}\frac{1}{\tilde{n}_x(w)\tilde{n}_y(w)}\right]^{\frac{1}{2}}\mathbb{E}\left[\mathbb{1}_{\{x\leftrightarrow y\}}\tilde{n}_x(w)\tilde{n}_y(w)\right]^{\frac{1}{2}}\\
&\leq \mathbb{E}\left[1_{\{x\leftrightarrow y\}}\frac{1}{\tilde{n}_x\tilde{n}_y}\right]^{\frac{1}{2}}P(x\leftrightarrow y)^{\frac{1}{2}-\frac{1}{2m}}\mathbb{E}\left[(\tilde{n}_x\tilde{n}_y)^{2m-1}\right]^{\frac{1}{2m}}\\
&\leq \mathbb{E}\left[1_{\{x\leftrightarrow y\}}\frac{1}{\tilde{n}_x\tilde{n}_y}\right]^{\frac{1}{2}}P(x\leftrightarrow y)^{\frac{1}{2}-\frac{1}{2m}}\mathbb{E}\left[\tilde{n}_x^{2m}\right]^{\frac{1}{2m+1}}\mathbb{E}\left[\tilde{n}_y^{2m}\right]^{\frac{1}{2m+1}}, \qquad (2.7)
\end{aligned}$$

From equation (2.5) we further observe that

$$\mathbb{E}\left[1_{\{x\leftrightarrow y\}}\frac{1}{\tilde{n}_x\tilde{n}_y}\right] \leq 2N\langle\varphi_x^1\varphi_y^1\varphi_x^2\varphi_y^2\rangle. \qquad (2.8)$$

Considering the fact that local times have finite moments, as shown in [23, Lemma 4.7],

$$\mathbb{E}\left[\tilde{n}_x^{2m}\right] \leq b, \qquad \forall x\in V, \qquad (2.9)$$

where $b = b(m, d, \beta, N) < \infty$, rearranging the terms in equation (2.7) and using (2.8) and (2.9), we deduce the lower bound with

$$c = \frac{1}{2N} b^{-\frac{1}{2m-1}}.$$

□

Proposition 2.4.1 says that spin-spin correlation $\langle \varphi_x^1 \varphi_y^1 \varphi_x^2 \varphi_y^2 \rangle$ and the connection probability $P(x \leftrightarrow y)$ behave essentially the same. It's then expected that in a phase with long-range order in the Spin O(N) model, a corresponding phase exists in the RPM loop soup where there is a positive probability of connection for vertices at arbitrary distance. In two dimensions, where we have proven there is no long-range order due to the Mermin–Wagner theorem 1.3.1, we thus expect that the probability $P(x \leftrightarrow y)$ decays to zero as the distance increases. This is in fact true, and the decay rate is at least algebraic. We can prove this by extending the McBryan–Spencer bound 1.4.1 to the mixed-component spin-spin correlation we have considered.

Proposition 2.4.2. For any $\beta \in \mathbb{R}_+$ and $N \in \mathbb{N}$ with $N > 1$, there exists $c = c(\beta, N) \in (0, 1)$ such that for any $x, y \in \mathbb{Z}^2$,

$$\lim_{L \to \infty} |\langle \varphi_1^x \varphi_1^y \varphi_2^x \varphi_2^y \rangle_{B_n, N, \beta}| \leq \frac{1}{8} \|x - y\|^{-c}.$$

Proof. We first consider the case $N = 2$ and fix $\beta \in \mathbb{R}_+$. We parametrize the unit sphere by angles such that $\varphi_x = (\cos \theta_x, \sin \theta_x)$, where $\theta_x \in [0, 2\pi)$ for any $x \in B_n$. Using trigonometric identities, the invariance of the measure under simultaneous rotation of all spins, and the fact that $|\mathrm{Re}(z)| \leq |z|$ for all $z \in \mathbb{C}$, we obtain that any $x, y \in B_n$,

$$\begin{aligned} \left| \langle \varphi_x^1 \varphi_y^1 \varphi_x^2 \varphi_y^2 \rangle_{B_n, \beta} \right| &= \frac{1}{8} \left| \langle \cos(2(\theta_x - \theta_y)) - \cos(2(\theta_x + \theta_y)) \rangle_{B_n, \beta} \right| \\ &= \frac{1}{8} \left| \langle \cos(2(\theta_x - \theta_y)) \rangle_{B_n, \beta} \right| \\ &\leq \frac{1}{8} \left| \langle e^{2i(\theta_x - \theta_y)} \rangle_{B_n, \beta} \right|. \end{aligned}$$

The derivation of the upper bound and the generalization to $N \geq 3$ now follows analogously to the proof of 1.4.1. □

Chapter 3

Markov Chain

In this chapter we define a Markov Chain with the goal of simulating the zero-field RPM. We work with an equivalent reformulation of the model, so we start by redefining the state space and the modified measure, making this chapter self contained. We then provide a characterization of the state space as the union of edge-disjoint cycles, making use of Euler's theorem for multigraphs. Following this, we introduce a set of simple local transformations and prove their capability to construct any state, starting from the empty state and vice versa. These transformations are then employed to define an irreducible, aperiodic and reversible Markov Chain, converging to our chosen invariant distribution.

3.1 The space of link configurations and pairings

Definition 3.1.1. Let $G = (V, E)$ be a simple graph. A *link configuration* on G is an edge function $m : E \to \mathbb{N}$ such that $\forall x \in V$ we have $\sum_{y \sim x} m_{x,y} \in 2\mathbb{N}$.

The vertex set for a square lattice G in $\mathbb{Z}^2$ is defined as $V_n = \{(i, j) | i, j \in \{0, \dots, n-1\}\}$. The edge sets are defined differently for each boundary condition:

- **For Free Boundary Conditions:** E_n^f includes edges that connect adjacent vertices within the lattice, explicitly excluding edges that would connect the lattice's boundary vertices to the opposite side.
- **For Periodic Boundary Conditions:** E_n^p includes all edges in E_n^f plus additional edges that connect the boundary vertices of the lattice across to the opposite side, creating a toroidal topology.

In the case of periodic boundary conditions we can identify any square s with one of its vertices, for example the top-right one, this implies that the number of squares is $|V_n| = n^2$. With free boundary conditions the number of squares is $(n-1)^2$.

In the case of free boundary conditions the graph has an interior boundary $\partial^{in} V \subseteq V_n$, which is the set of vertices of degree less than 4 in (V_n, E_n^f).

Definition 3.1.2. A *multicolor link configuration* of N colors is a tuple $(m^1, \dots, m^N)$ of link configurations.

Note that the parity constraints are independent for each color. We will now simply refer to them as link configurations and call single-color configuration as monochromatic. Given a graph G, we denote the set of all its link configurations as $\Sigma = \Sigma_G$.

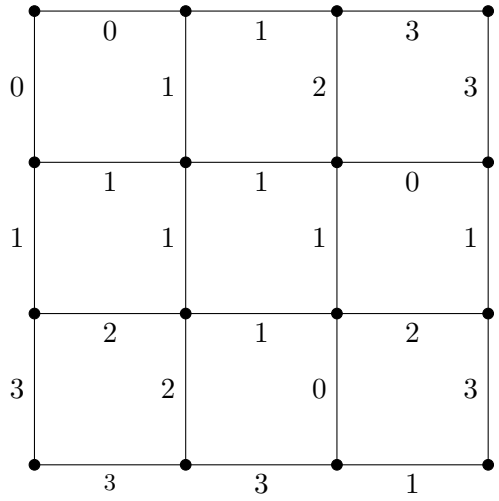

Figure 3.1. A grid of size $n = 4$ with free boundary conditions. Each edge is labelled with the value m_e of a link configuration m.

Given a link configuration, there is a natural way of building a multigraph $G_m = (V_n, E_m)$: use the value m_e as the number of times the edge e appears in the edge multi-set E_m of the multigraph. To avoid confusion with the original graph G, we refer to edges in the multigraph as links. The advantage of working with a multigraph is that statements like "the link configuration m contains a cycle" make sense now. When it doesn't cause confusion, we will refer to a link configuration and its associated multigraph as m.

Definition 3.1.3. A *pairing* for a link configuration m is a collection of partitions of the set of links of the same color incident to a vertex, such that every set in the partition has exactly two elements.

In simpler terms, at each vertex we are pairing links of the same color. By doing so, we are in fact partitioning the whole link set in circuits, which we will refer to as loops. We denote the set of all possible pairing configurations of a link configuration m as $\mathcal{P}(m)$. Our state space will be the set $\Omega := \{(m, \pi) : m \in \Sigma, \pi \in \mathcal{P}(m)\}$.

3.2 Edge-disjoint cycle representation

Consider a monochromatic state m. As pointed out in the preceding section, we can view it as a multigraph. Then the parity constraint in the definition of a link configuration is equivalent to requiring that the multigraph has even degree on all vertices. By Euler's theorem for multigraphs, we can represent m as a union of edge-disjoint cycles.

Lemma 3.2.1. Let $G = (V, E)$ be a multigraph with non-empty edge set, such that $\forall x \in V\ d(x) \in 2\mathbb{N}$. Then G contains a cycle.

Proof. Since $|E| > 0$, there exists a vertex $v \in V$ such that $d(v) \geq 2$. Starting from this vertex, choose any edge, say $\{v, x_1\}$. Since $d(x_1)$ is even, there exists at least one more unvisited edge incident to x_1. We continue this process iteratively, exploring unvisited edges and vertices. Since V is a finite set, after a finite number of steps, we must encounter a vertex that has already been visited: we have found a cycle. □

Proposition 3.2.1. If $G = (V, E)$ is a multigraph in which $\forall v \in V\ \deg(v) \in 2\mathbb{N}$, then the edge set E can be partitioned into edge-disjoint cycles.

Proof. We prove it by strong induction on the number of cycles. The base case is a multigraph with $|E| = 0$. Such a graph consists of one or more isolated vertices and the (empty) edge set can clearly be partitioned into a union of zero cycles.

Now suppose the result is true for every multigraph $G = (V, E)$ with $|E| \leq m$ edges whose vertices all have even degree. Consider a multigraph with $|E| = m + 1$. From Lemma 3.2.1 we know that there is at least one cycle $C = (\mathcal{V}, \mathcal{E})$ contained in G. Then we can form a new graph $G' = (V, E')$ by removing the edges that appear in the cycle $E' := E \setminus \mathcal{E}$. Every vertex in the cycle has its degree reduced by two, vertices that didn't appear in the cycle maintain the same degree: parity is preserved. Since we removed at least two edges (the shortest cycle possible in a multigraph) $|E'| \leq m$ so that by the induction hypothesis we can partition the edge set of G' as disjoint cycles $E' = \bigcup_{i=1}^{N} C_i$. Then adding C to the partition of E' we obtain a partition for the original edge set E. □

3.3 Square transformations

We define a class of transformations that map a state m to a new state m' by modifying only the links within a given square of the two dimensional square lattice. We limit ourselves to these transformations due to their local nature. Since our goal is to simulate a Markov chain on Σ, locality ensures that the exploration of the state space remains computationally tractable.

Definition 3.3.1. Given a square $s = (e_1, e_2, e_3, e_4)$ and four integers $\alpha_1, \alpha_2, \alpha_3, \alpha_4$ with the same parity, we define the *square transformation*

$$X_{s,(\alpha_1,\alpha_2,\alpha_3,\alpha_4)} : S \subseteq \Sigma \to \Sigma$$

that sends a state m to a new state m' defined by

$$m'_e = \begin{cases} m_{e_i} + \alpha_i & \text{if } e = e_i\ , \\ m_e & \text{otherwise.} \end{cases}$$

The domain S of the square transformation is defined to ensure the absence of negative links after applying the transformation:

$$S := \{m \in \Sigma \mid m_{e_i} \geq \alpha_i,\ \text{for } i = 1, 2, 3, 4\}$$

Each square transformation is characterized by the square it acts on and the four integers associated with it. We will ofter represent them using the square diagram in figure 3.2:

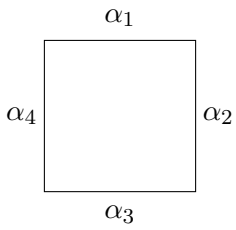

Figure 3.2. The diagram of the square transformation $X_{s,(\alpha_1,\alpha_2,\alpha_3,\alpha_4)}$.

The parity constraints on these integers ensure that the parity number of links incident at each vertex is preserved since in accordance with definition 3.1.1.

Given that our state is generally a multicolor link configuration, we require a distinct set of square transformations for each of the possible N colors, each acting only on a single color. When needed, we will explicitly indicate the color on which a transformation acts as $X_{s,c}$ with $c = 1, \ldots, N$. A general square transformation will be denoted simply as X_s.

We now define a special set of square transformations. The first U^{+1} is called *uniform* $+1$. Then we define four called *single* transformations, one for side of the square: R^{-2}, L^{-2}, T^{-2}, and B^{-2}, corresponding to *right, left, top,* and *bottom*, respectively. The associated integers for these transformations are presented in Table 3.1, their diagrams are depicted in figure 3.3.

U^{+1}	$(+1, +1, +1, +1)$
T^{-2}	$(-2,\ 0,\ 0,\ 0)$
R^{-2}	$(\ 0, -2,\ 0,\ 0)$
B^{-2}	$(\ 0,\ 0, -2,\ 0)$
L^{-2}	$(\ 0,\ 0,\ 0, -2)$

Table 3.1. Associated integers of uniform and single square transformations.

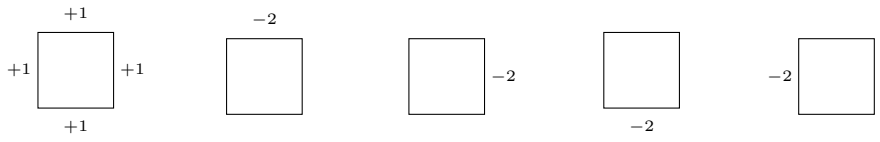

Figure 3.3. Diagrams of square transformations U^{+1}, T^{-2}, R^{-2}, B^{-2}, and L^{-2}, from left to right.

The importance of this set of square transformation resides in the following proposition:

Proposition 3.3.1. All square transformations can be obtained by composing uniform $+1$ and single -2 transformations.

Proof. Let X_s denote any square transformation, and let $\alpha_1, \alpha_2, \alpha_3, \alpha_4$ be its associated integers. Since they have the same parity, we can always find non-negative integers $k, \beta_1, \beta_2, \beta_3, \beta_4$ such that:

$$\begin{cases} \alpha_1 = k - 2\beta_1 \\ \alpha_2 = k - 2\beta_2 \\ \alpha_3 = k - 2\beta_3 \\ \alpha_4 = k - 2\beta_4 \end{cases}$$

We can use these integers to get the following decomposition:

$$X_s = L_s^{\beta_4} \circ B_s^{\beta_3} \circ R_s^{\beta_2} \circ T_s^{\beta_1} \circ U_s^k$$

where the composition is defined as $R_s^n := R_s^{-2} \circ \cdots \circ R_s^{-2}$ n times.

□

Remark 3.3.1. In the case of periodic boundary conditions, we actually only need single -2 transformations for vertical and horizontal edges, meaning we can use just U^{+1}, T^{-2} and R^{-2} to obtain any square transformation.

If we use these set of transformation in the case of free boundary conditions, to have completeness we also need to include L^{-2} and B^{-2} when we are at the left and bottom border respectively.

3.4 State construction

We will demonstrate two key properties of square transformations:

1. For free boundary conditions, it is possible to construct any link configuration starting from the empty state (zero links on all edges) and vice versa, using only a sequence of uniform $+1$ and the four single -2 transformations.

2. For periodic boundary conditions, such a construction is impossible. This is obvious when we our grid has odd length sides, since we can find states with an odd number of links, but square transformation preserves the parity of the total number of links in a state. The general case will follow from the topological properties of the torus.

Proposition 3.4.1. Any state $m \in \Sigma_G$, where $G = (V_n, E_n^f)$ is a box subset of $\mathbb{Z}^2$ with free boundary conditions, can be constructed from the empty state $0 \in \Sigma_G$ by using uniform $+1$ and the four single -2 transformations. Moreover, with the same set of transformations one can also reach the empty state starting from any state. This means there exists sequences of transformations depicted in figure 3.3 $X_1, X_2, \ldots, X_k$ and $Y_1, Y_2, \ldots, Y_l$ such that:

$$0 \xrightarrow{X_1} m_1 \xrightarrow{X_2} m_2 \ \ldots \ m_{k-1} \xrightarrow{X_k} m, \qquad\qquad m \xrightarrow{Y_1} n_1 \xrightarrow{Y_2} n_2 \ \ldots \ n_{l-1} \xrightarrow{Y_l} 0$$

where $m_1, m_2, \ldots, m_{k-1} \in \Sigma$ and $n_1, n_2, \ldots, n_{l-1} \in \Sigma$ are intermediate states.

Proof. Since we can work with any color independently, we consider a monochromatic state without loss of generality.

Given that our state has even degree on all vertices of the lattice, we can apply proposition 3.2.1 on the multigraph G_m. Call the edge-disjoint cycle partition of the edges $\{C_i\}_{i\in[N]}$, where N is the number of cycles. Since the cycles are edge disjoint, we can construct them separately, thus we only need to prove that we can build a single cycle[1].

Constructing a cycle starting from the empty state is straightforward: the *interior*[2] $\mathrm{Int}(C)$ of a cycle C is defined as a subset of squares such that:

$$\mathrm{Int}(C) := \{s \mid \text{ any path from } s_v \text{ to } \partial G \text{ contains a vertex of } C\}$$

Recall that s_v is the set of vertices of square s and ∂G is the set of boundary vertices of the graph.

If the cycle has more than 2 edges (the cycle is a simple graph) apply the uniform $+1$ to every square in $\mathrm{Int}(C)$ (which is at least one square). Subsequently, eliminate the undesired double edges with the single link -2 transformations.
If the cycle has 2 edges (in this case the interior is empty), we can construct it by applying the uniform $+1$ transformation twice and then applying single -2 to eliminate the three undesired edges. □

Example 3.4.1. Suppose we want to build the red cycle in the left picture of figure 3.4.

1. Apply uniform $+1$ on all squares on the interior of the cycle.
2. Use single -2 to remove the double links inside.

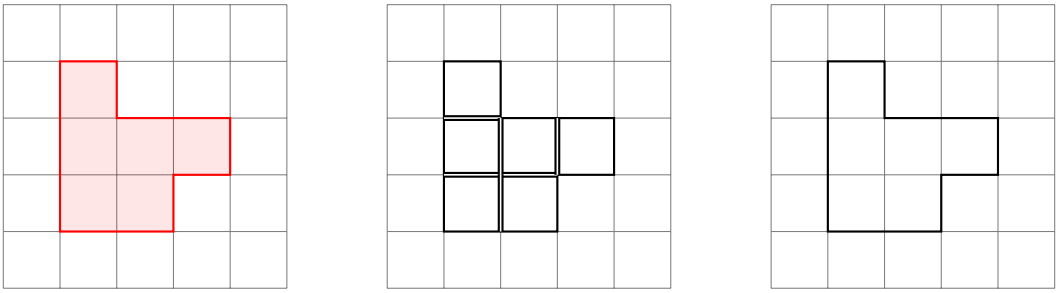

Figure 3.4. How to build/destroy any cycle with a well defined interior.

This procedure works on the plane, but not on the torus! In this case, the boundary ∂G is empty, and we can't define the interior/exterior of a closed curve as in the proof of Proposition 3.4.1. Still, there are some simple closed curves that separate the torus into two regions, both of which have the curve as a boundary. Clearly, we can build these curves using the same procedure applied to any of these two regions.

[1] This argument can be made precise through induction on N.
[2] Here the assumption of free boundary conditions is necessary.

However, this does not work in general. In fact, there exist closed curves that don't separate the torus into two regions, hence we can't apply the same procedure. We call these curves *non-separating*, see Figure 3.5.

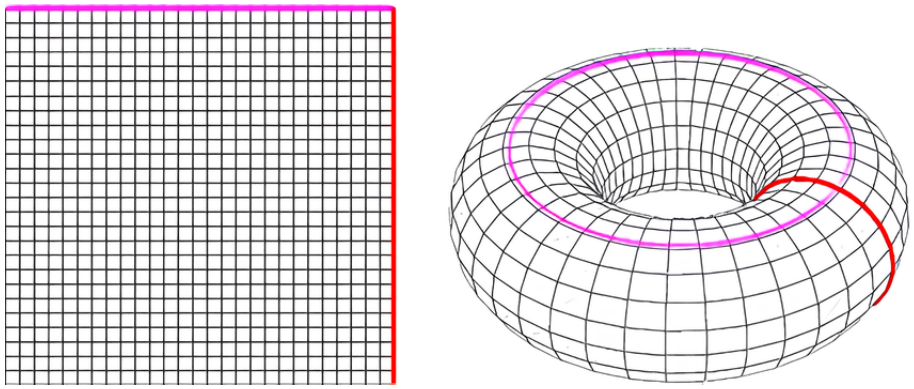

Figure 3.5. In pink an *horizontal non-separating* closed curve on the torus, in red a *vertical* one.

Being non-separating is a topological property, we will work with a characterization more suited for our setting.

We call an *horizontal ray* a simple closed curve on the torus that is parallel to horizontal links and does not intersect any vertex, like the curve in orange in figure 3.6. Their vertical counterpart is called *vertical ray*.

The characterization will exploit the fact that if a closed curve γ is separating, then the number of intersections with any horizontal and vertical ray l is even. We denote this number as $\mathrm{Cross}_l(\gamma)$.

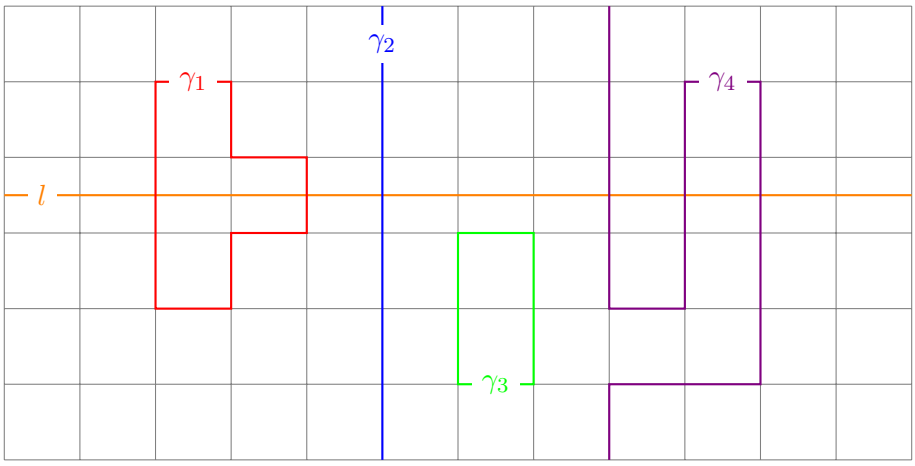

Figure 3.6. Four closed simple curves on the torus and an horizontal ray l in orange. Here $\mathrm{Cross}_l(\gamma_1) = 2$, $\mathrm{Cross}_l(\gamma_2) = 1$, $\mathrm{Cross}_l(\gamma_3) = 0$ and $\mathrm{Cross}_l(\gamma_4) = 3$.

Clearly if γ_1 and γ_2 are two edge-disjoint curves, then $\mathrm{Cross}_l(\gamma \cup \eta) = \mathrm{Cross}_l(\gamma) + \mathrm{Cross}_l(\eta)$, so that any separating circuit, which can be written as the union of edge-disjoint cycles (which are closed simple curves), has even cross number.

We call a non-separating closed curve γ *vertical non-separating* if there exists

an horizontal ray l such that $\text{Cross}_l(\gamma)$ is odd; we call it *horizontal non-separating* if the same is true for a vertical ray l. The curves γ_2 and γ_4 in figure 3.6 are both vertical non-separating.

Proposition 3.4.2. A closed curve γ on the torus is non-separating if and only if there exists a horizontal or vertical ray l such that $\text{Cross}_l(\gamma)$ is odd.

Proof. We will prove the equivalent statement: γ is separating if and only if $\text{Cross}_l(\gamma)$ is even for every horizontal or vertical ray l. This can be proven using an argument similar to the one used in proving Jordan's curve theorem for polygons.

Assume γ is separating. Let A and B be the two disjoint regions of the torus such that $\partial A = \partial B = \gamma$. Choose a point x on any given vertical or horizontal ray l which does not lie on γ. Then either $x \in A$ or $x \in B$. Suppose, without loss of generality, that $x \in A$. If $\text{Cross}_l(\gamma)$ were odd, then we would also have $x \in B$, contradicting $A \cap B = \emptyset$.

Now suppose that for any vertical or horizontal ray l, $\text{Cross}_l(\gamma)$ is even. We can then define two distinct subsets as follows:

1. Choose a point x at the center of a square s and a horizontal ray l that intersects x. Assign all points within square s to the set A.

2. Consider another square s' intersecting with l, and denote its center as x'. Divide ray l into two curves l_1 from x to x' and l_2 from x' to x. Since $\text{Cross}_l(\gamma)$ is even, the intersections of curves l_1 and l_2 with γ have the same parity. If it's even, assign all points in square s' to set A, otherwise to B.

3. Apply this procedure to the centers of the squares already assigned, using vertical rays to assign the remaining squares.

It's straightforward to verify that the sets $A \setminus \gamma$ and $B \setminus \gamma$ have the desired properties, hence γ is separating. □

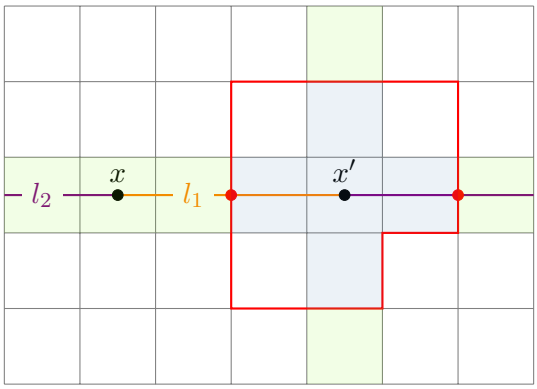

Figure 3.7. The procedure used to define the subsets A and B discussed in the proof of proposition 3.4.2. The number of intersection of both l_1 and l_2 is odd.

Proposition 3.4.3. Let $m \in \Sigma_G$ with $G = (V_n, E_n^p)$ be a state consisting of only separating curves. If, given a square transformation X_s, the new state $m' = X_s(m)$ contains a non-separating curve γ, then it contains exactly two non-separating curves.

Proof. We need to consider only transformations that add more links. By Proposition 3.3.1, any square transformation can be written using uniform $+1$ and single -2 transformations. Thus, we are left with only uniform $+1$: $X_s = U_s^{+1}$.

If the new state $m' = U_s^{+1}(m)$ contains a non-separating curve γ, then one or two of its edges were introduced by the transformation. This means that in the original state m, all the vertices in γ were already in the same connected component H (a circuit is at least 2-connected). Then, by Euler's theorem for multigraphs, we can find in H a circuit C which visits every vertex in γ. If we remove the edges of any path P joining any two vertices in H, then $H \setminus P$ contains a path visiting all the remaining edges (an Eulerian path) joining the same vertices. We will employ this fact to build another non-separating curve.

Let e_1, e_2, e_3 and e_4 be the four new added links to square s, and x and y be the vertices of this square that were also in H. We can write the non-separating curve γ as the union of a path P_{xy} from x to y contained in the circuit H and one or two of the new edges:

$$\gamma = P_{xy} \cup \{e_1\} \qquad \text{or} \qquad \gamma = P_{xy} \cup \{e_1, e_2\}$$

Let $\tilde{P}_{xy}$ be the Eulerian path joining x to y contained in $H \setminus P_{xy}$. Then the closed curves

$$\tilde{\gamma} = \tilde{P}_{xy} \cup \{e_2, e_3, e_4\} \qquad \text{or} \qquad \tilde{\gamma} = \tilde{P}_{xy} \cup \{e_3, e_4\}$$

are also non-separating, since for any horizontal/vertical ray l:

$$\mathrm{Cross}_l(\tilde{\gamma}) = \mathrm{Cross}_l(C) - \mathrm{Cross}_l(\gamma)$$

where $\mathrm{Cross}_l(C)$ is even, since it's a circuit contained in the original state m, and $\mathrm{Cross}_l(\gamma)$ is odd since γ is non-separating, implying $\mathrm{Cross}_l(\tilde{\gamma})$ is also odd. □

A straightforward consequence of this proposition is that we cannot reach a state with an odd number of non-separating curves starting from the empty state, as they can only be produced in pairs. More generally:

Corollary 3.4.1. Each parity number of non-separating curves (vertical and horizontal) is invariant with respect to square transformations.

To overcame this problem we are forced to introduce new non square transformations that don't preserve the parity of non-separating curves, such as:

$$V_k^{+1}(m)_e := \begin{cases} m_e + 1 & \text{if } e \text{ connects two vertices on the vertical line } x = k \\ m_e & \text{otherwise} \end{cases}$$

$$H_k^{+1}(m)_e := \begin{cases} m_e + 1 & \text{if } e \text{ connects two vertices on the horizontal line } y = k \\ m_e & \text{otherwise} \end{cases}$$

Notice how we don't need their inverses, since we can apply them twice and then use the single -2 to remove all links. The downside is that they affect all the edges on a given vertical/horizontal line: they are not local, in the sense that the number of affected edges depends linearly on the size of the grid.

3.5 Transition probabilities

We define a probability measure on the set Ω, equivalent to the RPM measure (2.3) with $h = 0$.

$$\mathbb{P}(\omega) = \frac{1}{Z} \prod_{e\in E} \prod_{i=1}^{N} \frac{\beta^{m_e^i}}{m_e^i!} \prod_{x\in V} \frac{\Gamma(\frac{N}{2})}{2^{n_x(m)}\Gamma(\frac{N}{2} + n_x(m))} = \frac{1}{Z}\mu(m) \tag{3.1}$$

Where Z is a normalization constant, $\beta \in \mathbb{R}_{\geq 0}$, N is the number of colors and $n_x(m) := \sum_{i=1}^{N} n_x^i(m) = \sum_{i=1}^{N} \frac{1}{2} \sum_{y\sim x} m_{x,y}^i$ which we refer to as the *local time*.

Since it is independent of the pairing configuration, the marginal probability of link configurations is simply

$$\rho(m) = \sum_{\pi\in\mathcal{P}(m)} \mathbb{P}(m, \pi) = \frac{1}{Z}\mu(m)|\mathcal{P}(m)| \tag{3.2}$$

where the number of possible pairings configurations is

$$|\mathcal{P}(m)| = \prod_{x\in V} \prod_{i=1}^{N} (2n_x^i(m) - 1)!!$$

since the number of pairings of a given color at each vertex is the same as the number of perfect matchings in a complete graph $K_{2n_x^i(m)}$.

To sample from probability measure (3.1) we first sample from the marginal measure (3.2) and then uniformly sample a pairing configuration.

Definition 3.5.1. Let $m, m' \in \Sigma$. We say m and m' are neighbours, denoted by $m \sim m'$, if there exists a square transformation X_s^c such that $X_s^c(m) = m'$.

It is evident that the neighbourhood of a state depends upon the chosen set of square transformations. Further, to make the relation $\sim$ symmetric and the dynamics reversible, we need to include also the inverses of square transformations 3.3. Considering a starting state $m \in \Sigma$, we aim to transition to a neighbouring state m' with a given probability $q(m'|m)$ called *jump probability*.

A simple strategy is to choose uniformly at random a color, a square and a square transformation. A caveat arises when m' results from a -2 transformation: if the edge is not on the boundary of the lattice, there are two ways to transition to m', e.g., a T^{-2} transformation has the same effect of a B^{-2} transformation applied at the square above. To avoid this ambiguity, we exploit Remark 3.3.1 and consider only transformations U^{+1}, T^{-2}, R^{-2} for squares not adjacent to the left and bottom borders, while adding L^{-2} for square on the left and B^{-2} for squares on the bottom. This restriction ensures there is a unique combination of color, square, and transformation to reach a neighbouring state, simplifying the computation of the jump probability to:

$$q(m' \mid m) = \begin{cases} \frac{1}{N} \frac{1}{(n-1)^2} \frac{1}{\mathcal{M}_{s,c}(m)} & \text{if } m' = X_s^c(m), \\ 0 & \text{otherwise,} \end{cases}$$

where $\mathcal{M}_{s,c}(m)$ denotes the number of possible transformations of color $c \in \{1, \dots, N\}$ that can be applied to square s given the link configuration m, and $(n-1)^2$ is the total number of squares within the grid.

We look for transition probability of the form:

$$P(m \to m') = q(m' \mid m) A(m', m),$$

where $A(m', m)$ is called the *acceptance probability* from state m to state m'. Imposing the detailed balance equations, we find the condition

$$\frac{A(m', m)}{A(m, m')} = \frac{q(m \mid m')}{q(m' \mid m)} \frac{\rho(m')}{\rho(m)} = \frac{\mathcal{M}_{s,c}(m)}{\mathcal{M}_{s,c}(m')} \frac{\rho(m')}{\rho(m)} \tag{3.3}$$

A common choice which satisfies condition (3.3) is the Metropolis-Hastings acceptance probability [30]:

$$A(m', m) = \min\left(1, \frac{\mathcal{M}_{s,c}(m)}{\mathcal{M}_{s,c}(m')} \frac{\rho(m')}{\rho(m)}\right) \tag{3.4}$$

Another option is the Glauber acceptance probability [31]:

$$A(m', m) = \left(1 + \frac{\mathcal{M}_{s,c}(m')}{\mathcal{M}_{s,c}(m)} \frac{\rho(m)}{\rho(m')}\right)^{-1}$$

Since m and m' only differ by a transformation in one square s, we can compute efficiently the ratios $\rho(m')/\rho(m)$.
Putting it all together, in the case of Metropolis acceptance probability the transition probabilities are:

$$P(m \to m') = \begin{cases} \frac{1}{N} \frac{1}{(n-1)^2} \frac{1}{\mathcal{M}_{s,c}(m)} \min\left(1, \frac{\mathcal{M}_{s,c}(m)}{\mathcal{M}_{s,c}(m')} \frac{\rho(m')}{\rho(m)}\right) & \text{if } m' \sim m \\ \sum_{m'' \sim m} \frac{1}{N} \frac{1}{(n-1)^2} \frac{1}{\mathcal{M}_{s,c}(m)} \left[1 - \min\left(1, \frac{\mathcal{M}_{s,c}(m)}{\mathcal{M}_{s,c}(m'')} \frac{\rho(m'')}{\rho(m)}\right)\right] & \text{if } m = m' \\ 0 & \text{otherwise} \end{cases} \tag{3.5}$$

The probability $P(m \to m)$ is defined to ensure the transition matrix is stochastic:

$$\sum_{m' \in \Sigma} P(m \to m') = \frac{1}{N} \frac{1}{(n-1)^2} \sum_{m' \sim m} \frac{1}{\mathcal{M}_{s,c}(m)} \tag{3.6}$$

$$= \frac{1}{N} \frac{1}{(n-1)^2} \sum_{s} \sum_{m' = X_s(m)} \frac{1}{\mathcal{M}_{s,c}(m)} \tag{3.7}$$

$$= \frac{1}{N} \frac{1}{(n-1)^2} \sum_{s} N = 1 \tag{3.8}$$

We can compute the explicit the probability ratios used in the acceptance probability for each of our possible neighbours.

Transition	Probability Ratio $\rho(m')/\rho(m)$
$m' = U^{+1}_{s,c}(m)$	$\frac{\beta^4}{16}\prod_{e\in s}(m^c_e+1)^{-1}\prod_{x\in s_V}\frac{2n^c_x(m)+1}{\frac{N}{2}+n_x(m)}$
$m' = U^{-1}_{s,c}(m)$	$\frac{16}{\beta^4}\prod_{e\in s}m^c_e\prod_{x\in s_V}\frac{\frac{N}{2}+n_x(m)-1}{2n^c_x(m)-1}$
$m' = R^{+2}_{s,c}(m)$	$\frac{\beta^2}{4(m^c_{e_2}+2)(m^c_{e_2}+1)}\prod_{x\in e_2}\frac{2n^c_x(m)+1}{\frac{N}{2}+n_x(m)}$
$m' = R^{-2}_{s,c}(m)$	$\frac{4m^c_{e_2}(m^c_{e_2}-1)}{\beta^2}\prod_{x\in e_2}\frac{\frac{N}{2}+n_x(m)-1}{2n^c_x(m)-1}$

Table 3.2. Probability ratios used to compute the acceptance probability.

3.6 Irreducibiliy

The key ingredient to show irreducibility of the Markov Chain with state space Σ and transition probabilities (3.5) is proposition 3.4.1, which asserts that in the case of free boundary conditions, any link configuration can be constructed starting from the empty state by applying the uniform $+1$ and single link -2 transformations and vice versa.

Remark 3.6.1. If m and m' are neighbours, then the transition probabilities $P(m \to m')$ and $P(m' \to m)$ are strictly positive. This follows from the definition of the acceptance probability and the fact that the probability measure (3.2) is strictly positive on all states.

Proposition 3.6.1. The Markov Chain with state space Σ_G with $G = (V_n, E^f_n)$ and transition probabilities (3.5) is irreducible.

Proof. Let $m, m' \in \Sigma$ be any states. By Proposition 3.4.1 and Remark 3.3.1, there exists a sequence of transformations $X_1, X_2, \ldots, X_k$ such that $0 \xrightarrow{X_1} m_1 \xrightarrow{X_2} m_2 \ldots \xrightarrow{X_k} m'$, where $m_1, m_2, \ldots, m_{k-1} \in \Sigma$ are intermediate states. By Remark 3.6.1, each transformation X_i has a positive probability. Therefore, the probability of the sequence is also positive since it is the product of positive numbers, this implies that $P(0 \to m') > 0$.

Similarly, by Proposition 3.4.1, there exists a sequence of transformations $Y_1, Y_2, \dots, Y_l$ such that $m \xrightarrow{Y_1} n_1 \xrightarrow{Y_2} n_2 \dots \xrightarrow{Y_l} 0$, where $n_1, n_2, \dots, n_{l-1} \in \Sigma$ are intermediate states. By Remark 3.6.1 and the same reasoning $P(m \to 0) > 0$, which together with $P(0 \to m') > 0$ implies that $P(m \to m') > 0$. □

3.7 Aperiodicity

Since the chain is irreducible, we only need to prove that a state has period one. By our choice of transition probabilities, if we can always find a state m and one of its neighbors m' such that the acceptance probability $A(m, m')$ is strictly less than one, then one can deduce from (3.5) that $P(m \to m) > 0$, ensuring that state m has period one.

Proposition 3.7.1. For any fixed $\beta > 0$ there exists a state $m \in \Sigma$ such that $A(m', m) < 1$ where $m' = U^{+1}(m)$.

Proof. By the definition of acceptance probability (3.4), we need to check

$$\frac{\rho(m')}{\rho(m)} \frac{\mathcal{M}_{s,c}(m)}{\mathcal{M}_{s,c}(m')} < 1$$

Since every transformation that we can apply at square s to state m can also be applied on state m', we have $\frac{\mathcal{M}_{s,c}(m)}{\mathcal{M}_{s,c}(m')} \leq 1$.

We can compute explicitly the probability ratio:

$$\frac{\rho(m')}{\rho(m)} = \frac{\beta^4}{16} \prod_{e \in s} (m_e^i + 1)^{-1} \prod_{x \in s_v} \frac{2n_x^i(m) + 1}{\frac{N}{2} + n_x(m)} \xrightarrow{m_e^i \to \infty} 0$$

so we can make the acceptance probability arbitrary small if we choose a state with enough links on the same edge. □

We end this chapter with a theorem that follows from all the previous results.

Theorem 3.7.1. The Markov Chain on the state space Σ_G with $G = (V_n, E_n^f)$ and transition probabilities (3.5) converges to the probability measure (3.2), regardless of the initial distribution.

Proof. Since the transition probabilities (3.5) where chosen to satisfy detailed balance equations with respect to measure (3.2), by a standard result [32, Lemma 1.9.2] this measure is invariant.

Since the chain is irreducible (Proposition 3.6.1) and aperiodic (Proposition 3.7.1), by a standard theorem [32, Theorem.1.8.3] we have convergence to its invariant probability measure regardless of the initial distribution. □

Chapter 4

Numerical simulations

This final chapter focuses on the implementation and numerical analysis of the Markov Chain defined in Chapter 3. We begin by outlining the challenges of Markov Chain Monte Carlo (MCMC), followed by a discussion of the code implementation and setup. We then study some observables: the number of links of each color, the covariance of local times, the lengths of the loops, the connectivity properties and percolation properties of the system.

4.1 Markov Chain Monte Carlo

Computing the probabilities of measure (2.3) requires calculating the partition function, a computationally intractable task for large systems. The only feasible approach to sample from this measure is to use a Markov Chain. The acceptance probabilities of our Markov Chain depend only on the ratio of probabilities, thus avoiding the need to compute the partition function; further, the chosen transformations are designed to ensure that the transition probabilities can be computed efficiently, since they rely only on local quantities (a single square of the lattice).

Supported by Theorem 3.7.1, our sampling strategy is as follows: start from any state, wait long enough to be close to the stationary measure and start sampling. A first question arises: *how long is long enough?* How can we tell how close are we to the stationary measure? The short answer is that we only have heuristics to asses convergence. A common strategy involves monitoring the trace of an observable, i.e. its value as a function of the steps of the chain, and wait long enough to see a stationary process (fluctuations from a fixed value).

Another heuristic utilized is the Gelman-Rubin diagnostic for multiple parallel chains [33], based on the following observation: if we run chains in parallel, then at equilibrium the variances within the chains and among different chains should be the same. Specifically, $\hat{R}$ is defined as the ratio of the estimated variance of the target distribution (accounting for both within-chain and between-chain variances) to the within-chain variance. When $\hat{R}$ is close to 1, it indicates that the chains have likely converged to the same distribution. Typically, values of $\hat{R} < 1.1$ are considered indicative of satisfactory convergence.

Another potential source of error is the *missing mass* problem. Even if the Markov chain is irreducible, it may take an exceptionally long time to explore certain

parts of the state space. One way to check if our chain is affected by this phenomenon is to start from different initial states and observe the time required to converge to a consistent value across runs. Another more direct approach is examining the transition probabilities for potential bottlenecks. The only solution to this problem is to add more possible jumps to improve mixing.

The last challenge in MCMC is that samples are correlated, which complicates the estimation of our estimator's variance.

Consider a Markov Chain $(X_n)_{n\geq 0}$ with state space Ω, and an observable $f : \Omega \to \mathbb{R}$. The estimator for the mean of $f(X)$ is defined as:

$$\hat{f} := \frac{1}{N}\sum_{n=1}^{N} f(X_n) \tag{4.1}$$

The variance of this estimator is given by:

$$\mathrm{Var}(\hat{f}) = \frac{1}{N^2}\sum_{k,n=1}^{N} \mathrm{cov}(f(X_k), f(X_n)) \tag{4.2}$$

Let σ_f^2 represent the variance of $f(X)$ with respect to the stationary distribution. For independent samples, the variance (4.2) is simply σ_f^2/N. However, in the presence of correlation, this variance is

$$\mathrm{Var}(\hat{f}) \approx \frac{\sigma_f^2\,\tau(f)}{N} \tag{4.3}$$

where the scaling factor $\tau(f)$, called the autocorrelation time of $f(X)$, is

$$\tau(f) := 1 + 2\sum_{n=1}^{\infty} \mathrm{cor}(f(X_0), f(X_n)) \tag{4.4}$$

If autocorrelation is high, to achieve good estimates we need more samples than the independent case.

4.2 Implementation and Setup

Code The chosen programming language is python, for its easy of use and vast external libraries. In addition to the standard Python libraries for mathematical operations and visualization, we also utilized the specific MCMC library ArviZ [34], which we used for variance estimation and to compute the Gelman-Rubin diagnostic.

To accelerate the simulation we used multi-core processing, running multiple chains in parallel—typically 8—and then combining the results.

All the code can be found on this GitHub repository, or can be imported into Python by installing the custom library PyRandomLoop.

Loop Sampling Recall that the state space of our chain consists only of colored link configurations. To sample a full state of the RPM model, we also need to sample a pairing configuration. The naive approach of randomly choosing pairings for all lattice vertices overlooks that the primary utility of these pairings is to construct loops: a pairings configuration is effectively a partition of the links into loops. We then use the following strategy: while there are vertices with positive local time

1. Pick a vertex x with non-zero local time n_x.
2. Select the next vertex y with probability proportional to the number of links on the edge xy, and remove one link on the crossed edge.
3. If y is the starting vertex x, close the loop with probability $(1+n_x)^{-1}$, otherwise return to step 2.

Eventually this process will halt and return a list of loops. Unfortunately, as β increases the number of links in the configurations increases, and the loop sampling procedure quickly becomes computationally intensive.

Extended Chain To improve mixing we introduce an additional set of square transformations. Early numerical experiments have identified a bottleneck: when β is small, the system typically features few links and small loops. If the chain starts from an initial state with lots of links, it struggles to eliminate long loops. This issue is supported by the observation that destroying a loop, as per procedure 3.4.1, initially requires applying U^{+1}. However, the probability of this event is proportional to β^4, making it exceedingly rare for $\beta \ll 1$. By introducing more transitions, we give the chain more ways to achieve this. We add a new set of transformations that swap links 4.1, meaning their acceptance probability does not depend on β. Note that all of these transformations can be derived from the previous ones by proposition 3.3.1; we introduce them solely to speed up convergence based on numerical experimentation.

Transition	**Probability Ratio** $\rho(m')/\rho(m)$
$m' = S^o_{s,c}(m)$	$\dfrac{m_{e_1} m_{e_3}}{(m_{e_2}+1)(m_{e_4}+1)}$
$m' = S^a_{s,c}(m)$	$\dfrac{m_{e_1} m_{e_2}}{(m_{e_3}+1)(m_{e_4}+1)} \dfrac{\left(\frac{N}{2}+n_{x_1}(m)-1\right)(2n^c_{x_3}(m)+1)}{\left(\frac{N}{2}+n_{x_3}(m)\right)(2n^c_{x_1}-1)}$

Table 4.1. Probability ratios for the new β-independent transitions used in the numerical simulations.

Figure 4.1. The square transformations S^a (left) and S^o (right).

Subsampling A straightforward strategy to reduce correlation between samples is subsampling: instead of sampling at every step, we sample at intervals of r steps:

$$\hat{f}_{\text{sub}} = \frac{1}{N/r} \sum_{n=1}^{N/r} f(X_{nr}), \tag{4.5}$$

where r is the subsampling interval. If r is chosen sufficiently large, the samples X_{nr} are nearly independent. However, by subsampling we are discarding lots of samples, and as a consequence of the Cauchy–Schwarz inequality, the variance in the subsampled case is greater.

But there's another practical reason why subsampling can be beneficial: when you take into account time. Ideally, we would like to choose r to minimize the error we get with a fixed amount of CPU time. Finding this optimal choice of r is non-trivial, a heuristic suggests setting r to the ratio τ_f/τ_{step}, where τ_f is the CPU time needed to sample the observable f and τ_{step} is the time needed for a simulation step. This ratio varies among the observables we study and depends on the grid size L and the value of β, ranging from 10 to 10^5.

4.3 Convergence and Equilibrium

In this section we try to establish if the chain converges and how long it takes to do so. As said before, we can only rely on heuristics and visual inspection of the trace plots of some chosen observables. The first test is to start the chain from different initial states, and check if they eventually agree. We choose four different states: the empty state (zero links), a random state obtained by applying random square transformations, and two manually crafted states called *snake* and *donut*, see Figure 4.2.

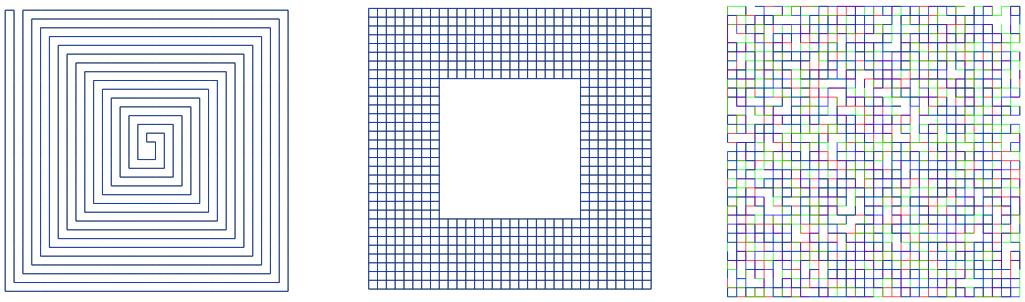

(a) **(b)** **(c)**

Figure 4.2. Three different initial 32×32 states: snake (a), donut (b) and random (c).

For this first test we study the trace plots of two loop observables: the mean loop length, and the length of the longest loop. We fix number of colors $N = 3$, the size of the lattice $L = 64$ and the inverse temperature $\beta = 2$.

As expected, the chain started with the snake state has initially the longest loops. Eventually an equilibrium is reached for the mean loop length, and all the chain agree regardless of the initial state Figure 4.3a. From the trace plot of the longest

loop length 4.3b we see that, even in the same chain, this observables exhibits huge variance. Nonetheless, if we compute the averages for each chain, we obtain similar results across chains, with an average value of 981 ± 36. The Gelman-Rubin statistic $\hat{R}$ is calculated to be 1.07, indicating that the chains have likely converged and are mixing well. From now on, we will start all numerical experiments from the empty state.

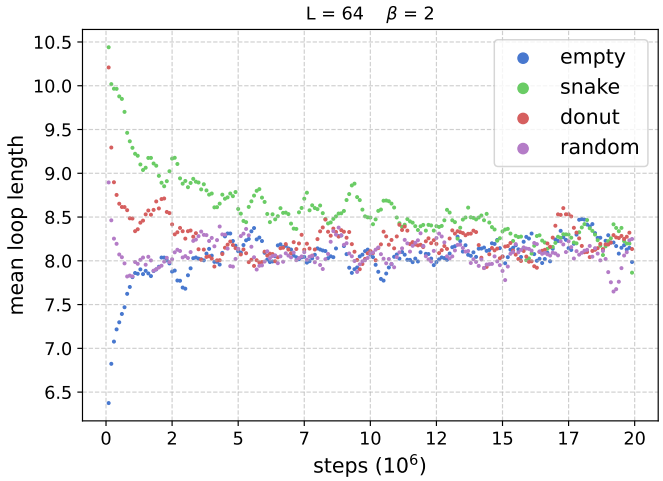

(a)

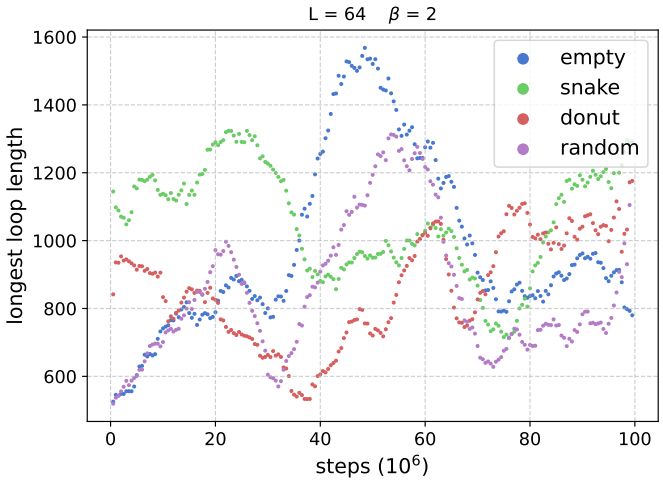

(b)

Figure 4.3. Trace plots of the chain started at different initial states. (a) Mean loop length. (b) Longest loop length (smoothed).

The next task is to obtain an estimate for the mixing time, when started from the empty state, and its dependence on the grid size L and the inverse temperature β. To do this, we study the trace plots of four observables: the mean number of links in the grid, the mean loop length, the connection probability between vertices at a distance of 8, and the longest loop length (precise definitions of these observables are provided in Subsection 4.4.4). We plot the trace plots of these observables,

normalized to their mean value across the last 100 samples, in Figure 4.4. Our observations are consistent with the findings in [21]: some observables take longer to reach equilibrium.

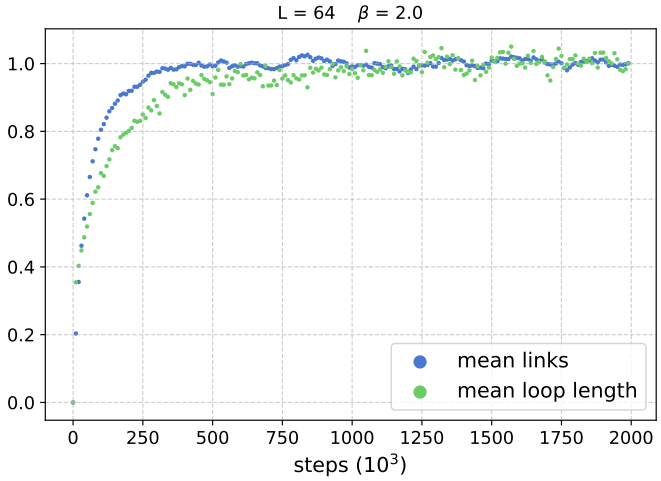

(a)

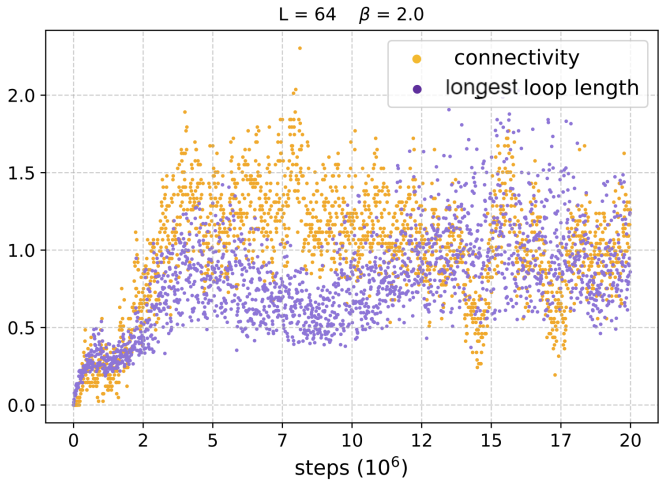

(b)

Figure 4.4. Trace plots of normalized observables for $L = 64$ and $\beta = 2.0$. (a) Mean links and mean loop length. (b) Connectivity and longest loop length.

Specifically, observables that depend on average quantities reach equilibrium at approximately $1 \cdot 10^6$ steps (see Figure 4.4a), whereas more complex observables require at least $5 \cdot 10^6$ steps (see Figure 4.4b). Furthermore, these complex observables exhibit high variance, thus requiring a large number of samples to obtain reliable estimates. To make things worst, these observables are computationally expensive since they rely on the pairings configuration.

The main observable we are interested in is the connection probability as a function of the distance, specifically its decay rate. If we start from the empty configuration, then we expect that at first only short loops are present, and slowly

longer loops start to appear: if we sample too early, then we might find a faster decay. To test this, we fix $N = 2$, $L = 64$, $\beta = 2$ and wait 50, 100, and 200 million steps before starting to sample. From Figure 4.5, we see that at 50 million steps convergence is not reached for big distances, showing a significantly faster decay. At 100 million steps convergence seems to be reached. We did the same test with the snake initial configuration, which starts biased with long loops, and again found that at 100 million steps equilibrium is reached.

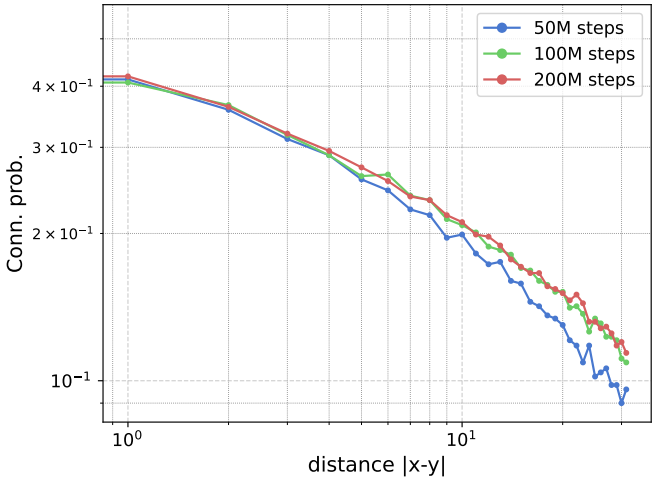

Figure 4.5. Connection probability for $N = 2$, $L = 64$ and $\beta = 2$, for various equilibrium steps before starting to take samples.

The expected behavior $T_{\text{mix}} \propto L^2$ is confirmed, as can be seen from Figure 4.6.

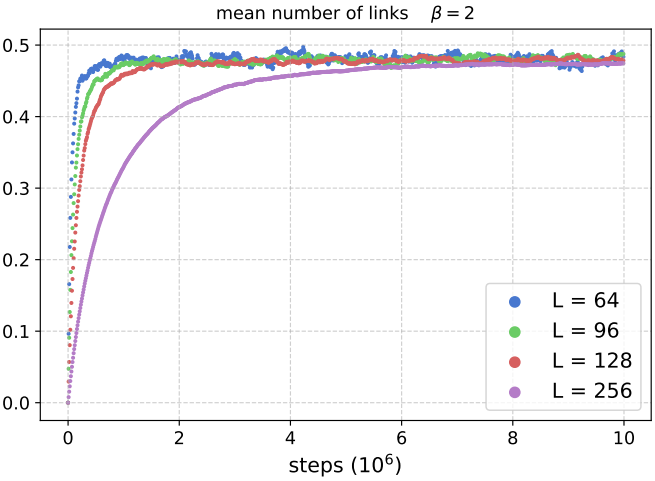

Figure 4.6. Trace plot of the mean number of links, for grid sizes $L = 64, 96, 128, 256$ and $\beta = 2$. Stationarity is reached at about $0.5 \cdot 10^6, 1 \cdot 10^6, 2 \cdot 10^6$ and $8 \cdot 10^6$, in agreement with $T_{\text{mix}} \propto L^2$.

The mixing time seems to be weakly dependant on the inverse temperature β, at

least for the range of inverse temperature we will study, which is $\beta \in [1, 4]$. The rationale for the lower bound is that at low β–high temperature– the system is not interesting: the lattice is mostly empty, only small loops of length 2 or 4 are present. Furthermore the high temperature region is when we have theoretical results about exponential decay of correlation. The system is interesting in the high β–low temperature–the lattice starts being populated and longer loops appear. Unfortunately, this also means that the loop sampling procedures slows, and that finite size effects begin to be significant.

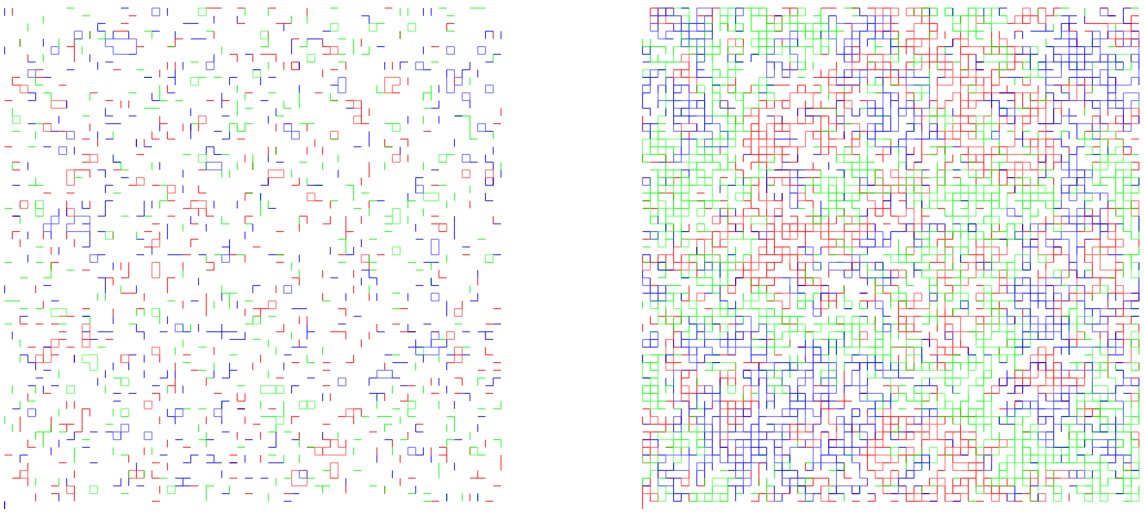

Figure 4.7. Link configurations with $N = 3$ and $L = 64$. Left: $\beta = 1$. Right: $\beta = 2$

In conclusion, we will wait at least 100 millions steps with $L = 64$ before starting to take samples. The scaled T_{mix} for each system size L are reported in Table 4.2.

L	T_{mix}	CPU time
64	$1 \cdot 10^8$	10 m
128	$4 \cdot 10^8$	40 m
256	$16 \cdot 10^8$	160 m
512	$64 \cdot 10^8$	10 h

Table 4.2. Approximate mixing time for various size of the lattice. The CPU used is a Ryzen 7 5800x, reaching about 180000 steps/s.

4.4 Analyzing Simulation Data

4.4.1 Links

The first observables we study are related to links. As can be seen in Figure 4.7, as the inverse temperature increases more links are present. If we remove interactions, i.e. set $U(n_x) = 1$, and ignore the parity constraints, the number of links on a single edge $m_e = \sum_{i=1}^{N} m_e^i$ is a Poisson random variable with parameter β, meaning $\langle m_e \rangle = N\langle m_e^i \rangle \simeq \beta$. Indeed for $N = 3$ and $L = 128$ we find the following linear relationship (Figure 4.8):

$$\langle m_e \rangle = c_1\beta + c_2, \qquad c_1 = 1.01230 \pm 10^{-5}, \quad c_2 = -0.5925 \pm 3 \cdot 10^{-4}.$$

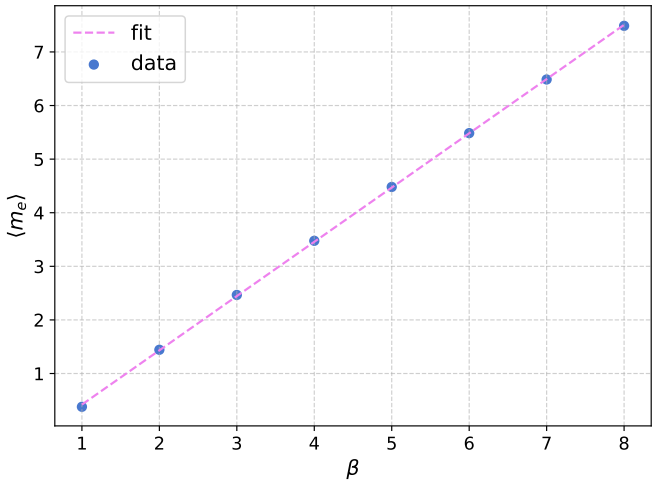

Figure 4.8. Mean number of links on a single edge as a function of β, for $L = 128$, 8000 samples for each point, $MCSE = 10^{-3}$.

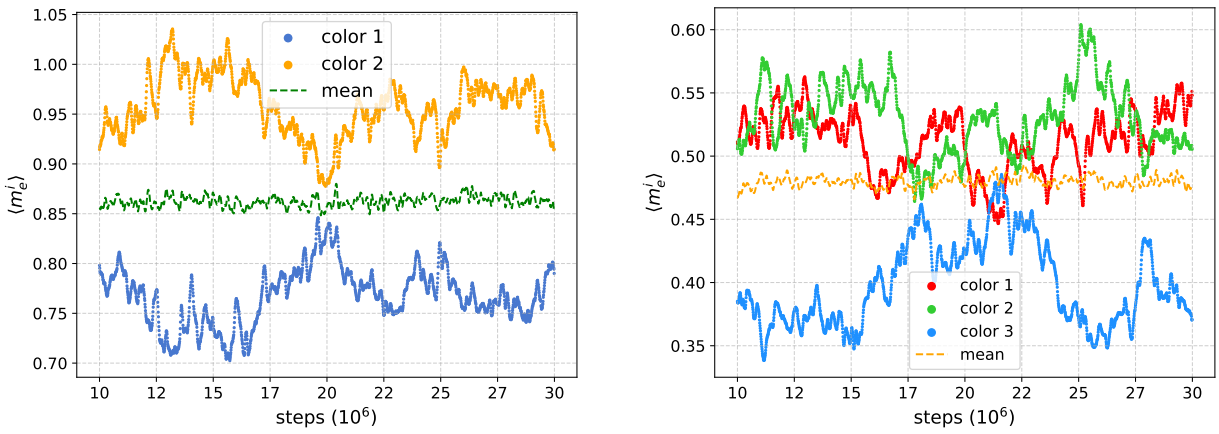

(a) **(b)**

Figure 4.9. Trace plots of the mean number of links of each color on a single edge for $L = 64$; (a) $N = 2$ the correlation coefficient is -0.87; (b) $N = 3$ the correlation coefficients are $-0.14, -0.55, -0.62$.

Since the interaction is repulsive, we expect links of different color to be anti-correlated. This is the case, see Figure 4.10a.

4.4.2 Local times

Since local times are a function of links, the same considerations of the previous subsection can be made: the average local time increase linearly with the inverse temperature, and local times of different colors are anti-correlated.

By inspecting link configurations, we find that links of the same color tend to cluster. We then expect that the local time of a color has some spatial coherence, meaning the correlation coefficient $\mathrm{corr}(n^1_x, n^1_y)$ is close to one for close vertices and decays to zero as the distance increases. Conversely, we expect that the correlation between local times of different colors starts negative, and then decays to zero as the distance increases. We numerically study the $N = 3$ case, in which the decay seems to be exponential $\mathrm{corr}(n^1_x, n^1_y) \sim e^{-|x-y|/\xi(\beta)}$ (Figure 4.10a). By doing a linear fit in log-scale we compute the correlation length ξ, which seems to increase linearly with the inverse temperature (Figure 4.10b).

$$\xi = c_1\beta + c_2, \qquad c_1 = 9.52 \pm 0.23, \quad c_2 = -10.66 \pm 0.33$$

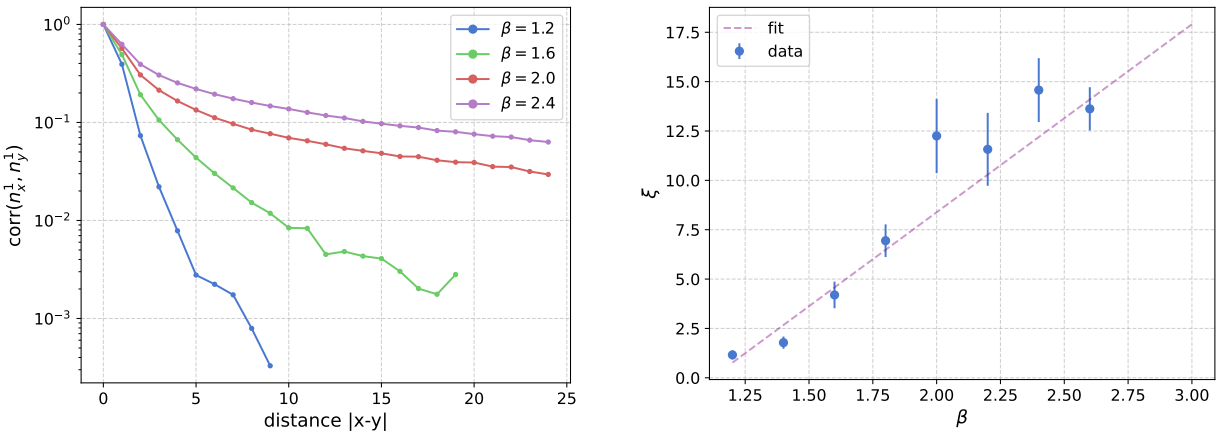

(a) **(b)**

Figure 4.10. (a) Correlation coefficient of local times of color 1, as a function of the distance. Data obtained with $L = 128$ and $2M$ samples for each point.; (b) Correlation length of local times of the same color as a function of the inverse temperature.

4.4.3 Loops

Obvious observables to study are the average and longest loop length. Unlike the previous two observables, these quantities rely on sampling pairing configurations, a computationally heavy procedure, especially for high β.

We observe that the average loop length increases linearly with β (Figure 4.11) and is weakly increasing with the system size L. This suggests that in two dimensions there isn't a positive density of macroscopic loops for any inverse temperature.

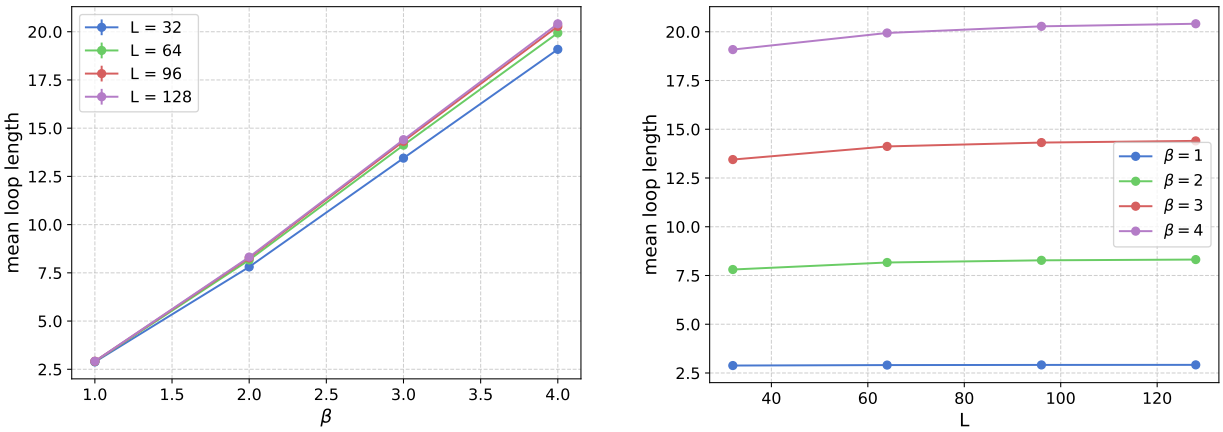

(a) **(b)**

Figure 4.11. Mean loop length as a function of β (a), of the system size (b).

A linear fit on the data from $L = 128$ yields a coefficient of 5.9 ± 0.1 and an intercept of -3.1 ± 0.3. The expected value of the longest loop scales algebraically with β and increases linearly with L (Figure 4.12).

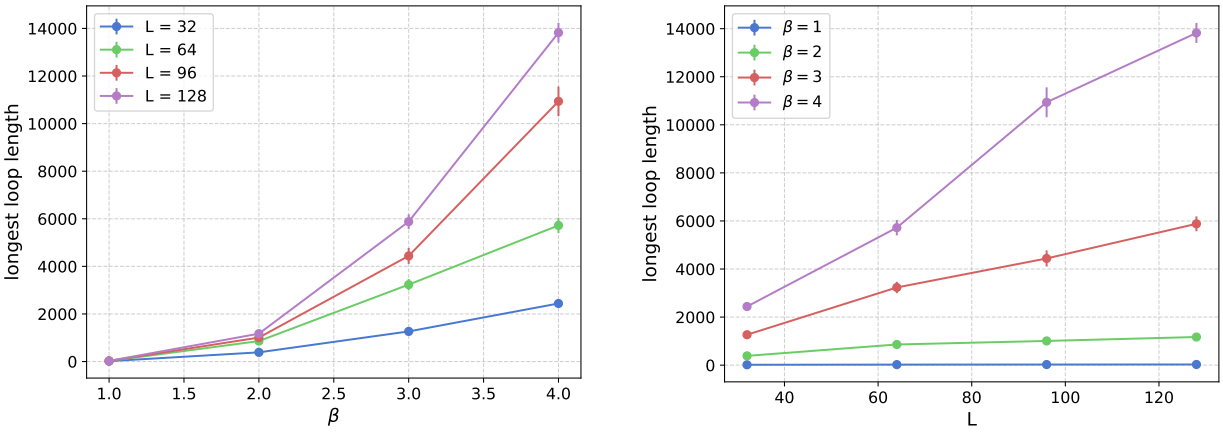

(a) **(b)**

Figure 4.12. Expected value of the longest loop as a function of β (a), of the system size L (b).

Fitting the data from $L = 128$ with the function ax^b yields $a = 124 \pm 19$ and $b = 3.12 \pm 0.11$.

The density of the longest loop, its length divided by the number of vertices, goes to zero as the size of the system increases (Figure 4.13), supporting the hypothesis that there is no positive density of macroscopic loops in the infinite volume limit.

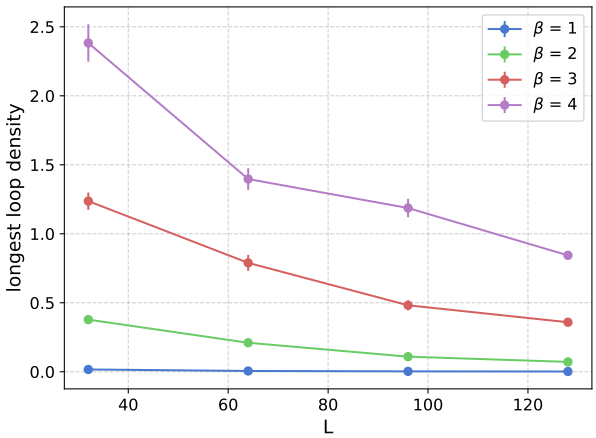

Figure 4.13. Density of the longest loop as a function of the system size L.

(a) $\beta = 1$

(b) $\beta = 2$

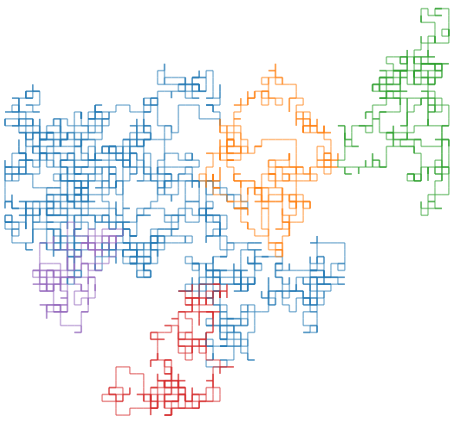

(c) $\beta = 3$

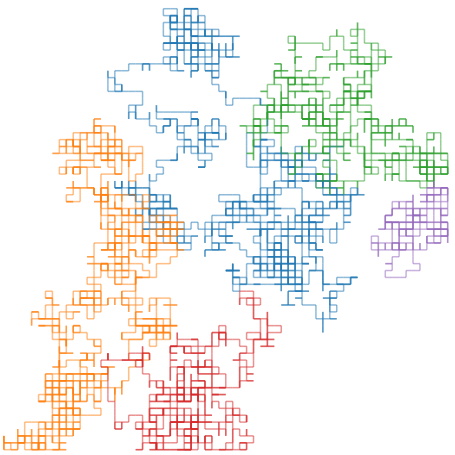

(d) $\beta = 4$

Figure 4.14. Longest loops with $L = 64$. (a) top 20 longest loops for $\beta = 1$; (b) top 8 longest loops for $\beta = 2$; (c) top 5 longest loops for $\beta = 3$; top 5 longest loops for $\beta = 4$.

4.4.4 Connection probability

We now estimate the connection probability of two vertices, meaning we pick two random vertices at a chosen distance and check if they are connected by a loop. This quantity is related to spin-spin correlation by Proposition 2.4.1, and by Proposition 2.4.2 we also expect that this probability decays to zero at least algebraically with the distance of the vertices. It is therefore interesting to study this decay, and look for a BKT phase transition.

To estimate this probability, given a link configuration we choose random pairs of vertices from distance 1 to $L/2$, and check if they are connected by a loop of color 1.

Since the BKT phase transition does not have a order parameter, it's subtle to detect. Our strategy is to plot this probability in both log and log–log scale: exponential decay should appear as a straight line in the former, algebraic decay in the latter.

Let $v(\ell)$ be the number of visited vertices of loop ℓ. Following [21], we define the observable

$$\nu(K) := \frac{1}{L^2} \sum_{\ell\,:\,|\ell|\geq K} v(\ell)$$

i.e. $\nu(K)$ is the sum of the fraction of visited vertices of loops of length greater or equal to K. In the case of random planar permutations this quantity is the probability that a vertex is contained in a loop of length $\geq K$, a quantity which decays algebraically if and only if the probability of two vertices being connected by a loop does. In our context this is not so clear, our definition of ν is even not normalized, since loops are not disjoint. The advantage of this observable is that it depends on the entire link configuration, and thus needs fewer samples to get good estimates. We can see from Figure 4.15 that from β bigger than 1.1 there seems to be a different behaviour, there is a straight line, signifying algebraic decay, while for lower β the curvature suggest exponential decay. This is clearer for the $\nu(K)$ observable.

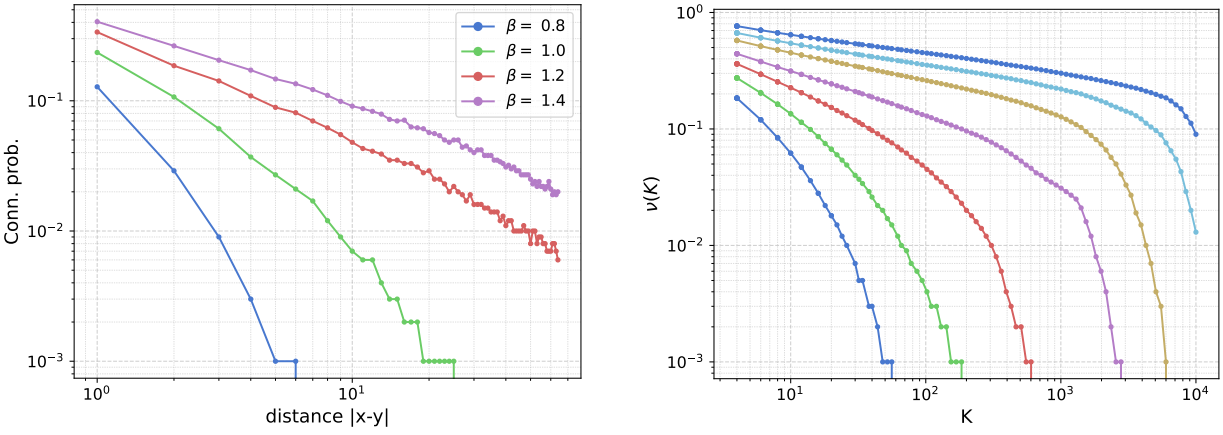

(a) **(b)**

Figure 4.15. log-log plot for $L = 128$ and $N = 2$ (a) connection probability as a function of the distance; (b) $\nu(K)$ with β from 0.8 to 1.4 in steps of 0.1.

To obtain a more quantitiative estimate on the phase transition, we study the behaviour of the power law decay and the exponential decay rate in the two phases, as a function of the inverse temperature.

Following the general theory of the BKT phase transition, above β_c in the phase of algebraic decay, to first approximation the power $p(\beta)$ with which correlations decay is linear in β^{-1}:

$$\nu(K) \sim K^{-p(\beta)}, \qquad p(\beta) \simeq c_1 \beta^{-1} + c_2$$

and the critical exponent $p(\beta_c)$ is known to be $1/4$, and is thought to be universal for all systems that exhibit a Kosterlitz-Thouless phase transition. By doing a linear fit in log-log scale we estimate the power $p(\beta)$, Figure 4.16. We find that the linear fit intersects the horizontal $1/4$ line at $\beta^{-1} = 0.867 \pm 0.054$, a value compatible with the estimate of the critical temperature of the XY model of $\beta_c^{-1} = 0.8929$ [35].

Below the critical inverse temperature, where the decay is exponential, the exponential decay rate $r(\beta)$ is expected to satisfy

$$\nu(K) \sim e^{-r(\beta)K}, \qquad r(\beta) \simeq c_1\, e^{-c_2|\beta^{-1}-\beta_c^{-1}|^{-1/2}} \tag{4.6}$$

By doing a linear fit in log scale to extract exponential decay rate $r(\beta)$, and fitting a function of the form (4.6), we find $\beta_c^{-1} = 0.88 \pm 0.07$, compatible with our previous estimate.

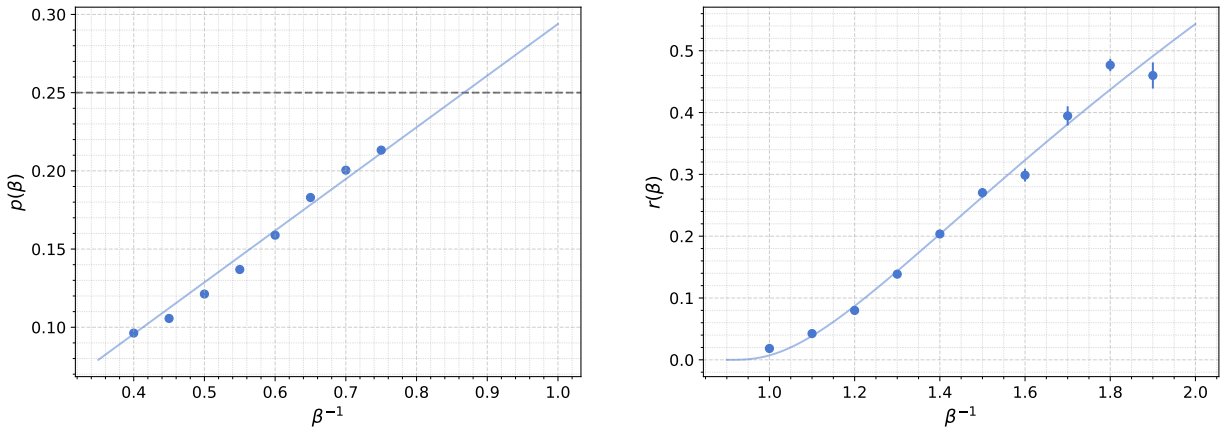

(a) **(b)**

Figure 4.16. (a) Algebraic decay coefficient $p(\beta)$ as a function of the temperature β^{-1}, in light blue a linear fit; (b) exponential decay rate $r(\beta)$ as a function of the temperature, in ligh blue best fit of (4.6).

For $N = 3$ the decays seems always exponential, Figure 4.17. The exponential decay rates $r(\beta)$ follow seems to be themselves exponential, see Figure 4.18.

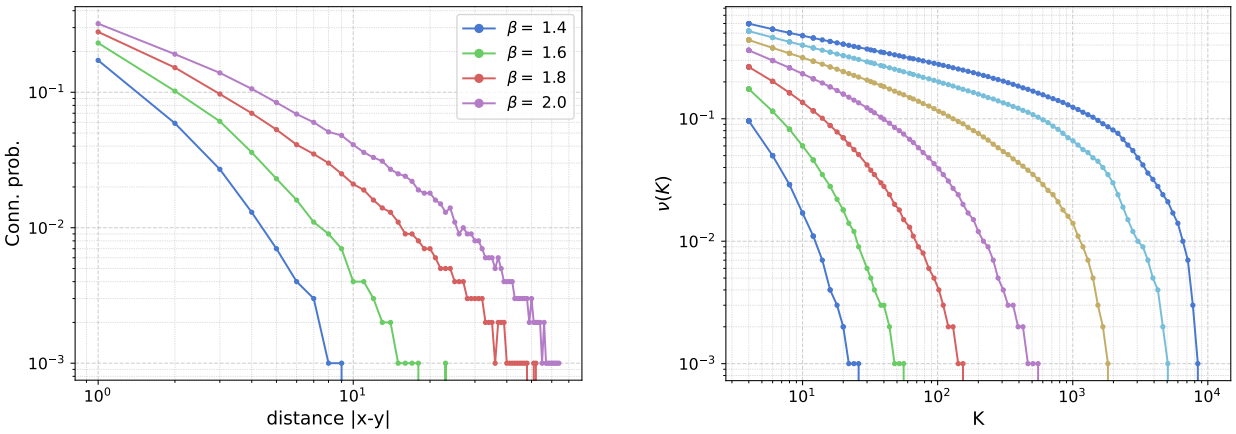

(a) (b)

Figure 4.17. log-log plot for $L = 128$ and $N = 3$ (a) connection probability as a function of the distance; (b) $\nu(K)$ with β from 1.0 to 2.2 in steps of 0.2.

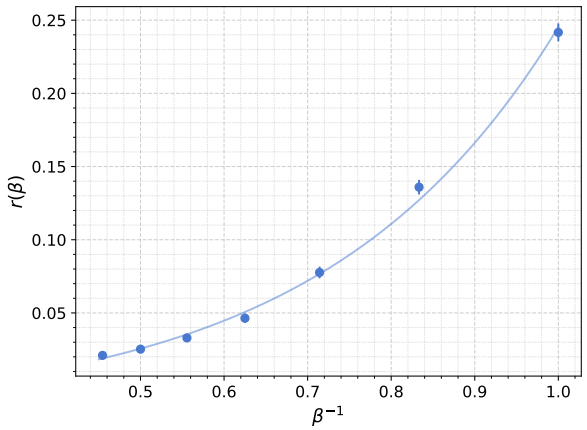

Figure 4.18. Exponential decay rate for the case $N = 3$ as a function of β^{-1}. The light blue curve is the exponential $c_1 e^{c_2/\beta} + c_3$ with $c_1 = 0.008 \pm 0.002$, $c_2 = 3.55 \pm 0.28$ and $c_3 = -0.019 \pm 0.008$.

4.4.5 Percolation

The trace of a link configuration $\hat{m}^c$ of color $c = 1, \ldots, N$, is defined as $\hat{m}^c := \{e \in E : m_e^c \geq 1\} \subseteq E$, i.e. the set of edges which contain at least one link. This trace appears in the switch Lemma used to relate the random current expansion to the probability of some event [29], specifically

$$\langle \sigma_x \sigma_y \rangle^2_{\Lambda,\beta,h} = P \otimes P[x \leftrightarrow y \text{ in } \widehat{n_1 + n_2}]$$

where $P \otimes P$ is the product of two independent distribution on sourceless currents (2.1). This equation show that in the Ising model long-range order gets rephrased into long-range connectivity in the sum of two sourceless currents, thus the infinite-volume version of $\widehat{n_1 + n_2}$ has an infinite connected component almost surely if and

only if $\beta > \beta_c$. It's still an open question whether this also holds for a single trace of a sourceless current. We will numerically study this question for the RPM loop soup with $N = 3$, even if we know there isn't a long-range order phase. To look for percolation, we check in the trace of a link configuration of one color if the left side of the lattice is connected with the right side using breadth first search. Indeed percolation occurs, see Figure 4.19.

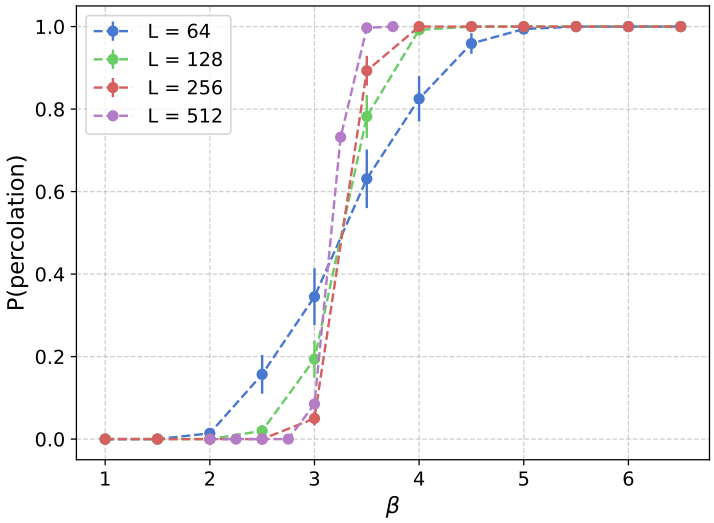

Figure 4.19. Percolation probability in the trace of a single color link configuration, for $N = 3$ as a function of the inverse temperature.

To estimate the percolation threshold, we follow the Yonezawa–Sakamoto–Hori method [36]: we first fit the data for each L to a sigmoid function, and then define the effective threshold $\beta_c^{perc}(L)$ to be when this function has value $1/2$. To extract the infinite volume threshold β_c^{perc}, we use the following scaling hypothesis:

$$\beta_c^{perc}(L) = \beta_c^{perc} + AL^{-1/\nu}, \qquad A, \nu \geq 0 \tag{4.7}$$

To estimate the critical exponent ν we make the scaling assumption

$$\partial_\beta P_\beta(\text{percolation}) \,|_{\beta=\beta_c^{perc}} \propto L^{-1/\nu}$$

i.e. that the derivative of the percolation probability at the critical inverse temperature diverges as a power law with the size of the system.

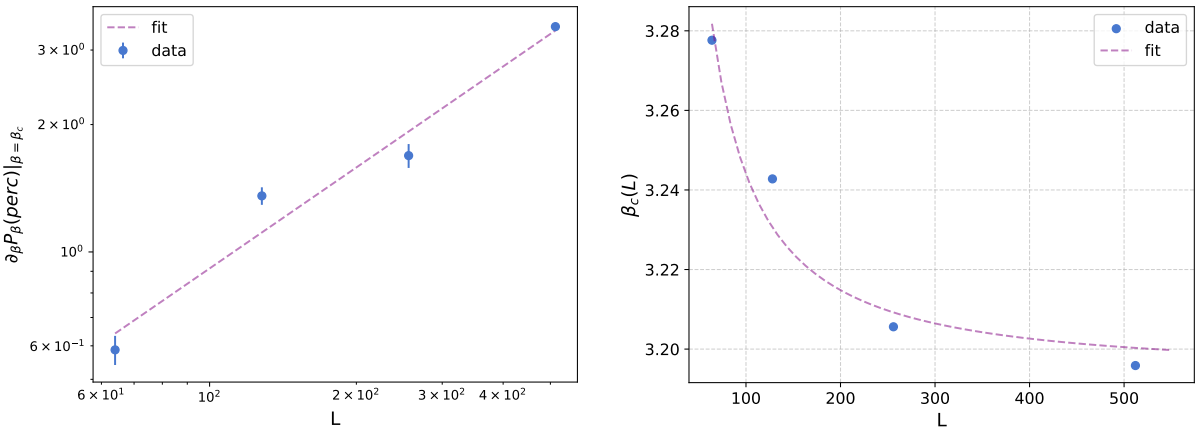

(a) **(b)**

Figure 4.20. (a) Derivative of the percolation probability at the effective critical value as a function of the system size. (b) effective percolation threshold as a function of L.

We estimate ν by doing a linear fit in log-log scale 4.20, and obtain the value $\nu = 1.26 \pm 0.19$ (for reference this exponent has a vale of $4/3 \approx 1.33$ for $2d$ bond percolation). By fitting the function (4.7), we find that the infinite volume percolation threshold is $\beta_c^{perc} = 3.19 \pm 0.01$.

Conclusion

The main goal of this thesis was to introduce a Markov Chain to simulate a loop soup model related to the classical Spin O(N) model. To motivate this study, we began by introducing the model, and proved known and important results about its behaviour, namely the Merming–Wagner theorem, which states that no spontaneous magnetization is possible for two dimensional models, and the McBryan–Spencer bound on the decay of spin-spin correlation.

We then moved to the random path representation introduced in [1], from which the random loop soup we intend to simulate has its origin. To provide context for this approach, we first briefly introduced the random currents expansion of the Ising model, of which the random path expansion is a generalization for continuous spins. We then proved some results that show why this representation is useful: spin-spin correlation can be reframed as loop connectivity (albeit non the standard spin-spin correlation, but a mixed component one). Known results about these models tell us that in two dimensions there is not a positive density of macroscopic loops, meaning that that connection probability decays to zero as the distance between vertices increases. After some work, we have shown that this decay is at least algebraic. Studying the decay of connection probability is one of the more interesting observable to investigate, since the it's not clear if the decay is always exponential, which is expected at high temperatures, or shows a BKT phase transition and becomes algebraic at low enough temperatures.

Finally we get to the original work of this thesis, the definition of the Markov Chain. The non trivial part of this endeavour was to develop a simple dynamics to explore the entire configuration space, a non trivial task due to the parity constraints of link configurations. Having achieved this with the introduction of square transformations, the transition probabilities of the chain were easily obtained using the standard Metropolis-Hastings procedure.

After some remarks about Markov Chain Monte Carlo and its challenges, we discussed the convergence of our chain, and found that only systems of sizes up 512 were in reach. Moreover, the strategy we employed, namely simulating a chain only on link configurations and only after sampling a pairing configuration, suffered numerical problems: the sampling procedure becomes computationally expensive as β increases, which is sadly the interesting low-temperature zone. For this reason we limited our numerical analysis to few values of β, and in a rather small range.

In general, the results from the numerical simulations were in line with our expectations: a linear dependence of the number of links/local times on the inverse temperature, and anti-correlation for different colors. The analysis of loop lengths was consistent with the theoretical results, showing no positive density of macroscopic

loops. We did observe a BKT phase transition at $\beta_c^{BKT} \simeq 1.15$ in the decay of loop connectivity for the $N = 2$ case , and an exponential decay at all inverse temperatures within our considered range for the $N = 3$ case. Interestingly, we observed a percolation phase transition at a critical inverse temperature $\beta_c^{perc} \simeq 3.19$ for $N = 3$, despite the lack of long-range order in two dimensions, in the trace of link configurations of a single color.

The main limitation of our approach was the high number of steps needed to reach equilibrium, which limited us to consider only rather small lattices. Further, the pairing sampling is a computationally expensive procedure. Perhaps there is a more complex Markov Chain which directly has pairings in its state space, and still runs faster, though proving irreducibly seems an harder problem. Due to this numerical difficulties, extending this approach to higher dimensional lattices seems to be not worth pursing, while the chain could be easily adapted to two dimensional lattices of different shapes, for example triangular or hexagonal. Generalizations to other loop soup models are straightforward.

Bibliography

[1] Benjamin Lees and Lorenzo Taggi. *Exponential decay of transverse correlations for O(N) spin systems and related models*. 2021. arXiv: 2006.06654 [math.PR].

[2] R. Peierls. "On Ising's model of ferromagnetism". In: *Mathematical Proceedings of the Cambridge Philosophical Society* 32.3 (1936), pp. 477–481. DOI: 10.1017/S0305004100019174.

[3] J J Hopfield. "Neural networks and physical systems with emergent collective computational abilities." In: *Proceedings of the National Academy of Sciences* 79.8 (1982), pp. 2554–2558. DOI: 10.1073/pnas.79.8.2554. eprint: https://www.pnas.org/doi/pdf/10.1073/pnas.79.8.2554. URL: https://www.pnas.org/doi/abs/10.1073/pnas.79.8.2554.

[4] Zhengbing Bian et al. "The Ising model: teaching an old problem new tricks". In: *D-wave systems* 2 (2010), pp. 1–32.

[5] H. E. Stanley. "Dependence of Critical Properties on Dimensionality of Spins". In: *Phys. Rev. Lett.* 20 (12 Mar. 1968), pp. 589–592. DOI: 10.1103/PhysRevLett.20.589. URL: https://link.aps.org/doi/10.1103/PhysRevLett.20.589.

[6] Lars Onsager. "Crystal Statistics. I. A Two-Dimensional Model with an Order-Disorder Transition". In: *Phys. Rev.* 65 (3-4 Feb. 1944), pp. 117–149. DOI: 10.1103/PhysRev.65.117. URL: https://link.aps.org/doi/10.1103/PhysRev.65.117.

[7] N. D. Mermin and H. Wagner. "Absence of Ferromagnetism or Antiferromagnetism in One- or Two-Dimensional Isotropic Heisenberg Models". In: *Phys. Rev. Lett.* 17 (22 Nov. 1966), pp. 1133–1136. DOI: 10.1103/PhysRevLett.17.1133. URL: https://link.aps.org/doi/10.1103/PhysRevLett.17.1133.

[8] J. Fröhlich, B. Simon, and Thomas Spencer. "Infrared bounds, phase transitions and continuous symmetry breaking". In: *Communications in Mathematical Physics* 50.1 (1976), pp. 79–95.

[9] Oliver A McBryan and Thomas Spencer. "On the decay of correlations in SO (n)-symmetric ferromagnets". In: *Communications in Mathematical Physics* 53 (1977), pp. 299–302.

[10] Ron Peled and Yinon Spinka. "Lectures on the spin and loop O (n) models". In: *Sojourns in Probability Theory and Statistical Physics-I: Spin Glasses and Statistical Mechanics, A Festschrift for Charles M. Newman*. Springer, 2019, pp. 246–320.

[11] V. L. Berezinsky. "Destruction of Long-range Order in One-dimensional and Two-dimensional Systems Possessing a Continuous Symmetry Group. II. Quantum Systems." In: *Sov. Phys. JETP* 34.3 (1972), p. 610.

[12] J M Kosterlitz and D J Thouless. "Ordering, metastability and phase transitions in two-dimensional systems". In: *Journal of Physics C: Solid State Physics* 6.7 (Apr. 1973), p. 1181. DOI: 10.1088/0022-3719/6/7/010. URL: https://dx.doi.org/10.1088/0022-3719/6/7/010.

[13] Jürg Fröhlich and Thomas Spencer. "The Kosterlitz-Thouless transition in two-dimensional abelian spin systems and the Coulomb gas". In: *Communications in Mathematical Physics* 81.4 (1981), pp. 527–602.

[14] Alexander M Polyakov. "Interaction of goldstone particles in two dimensions. Applications to ferromagnets and massive Yang-Mills fields". In: *Physics Letters B* 59.1 (1975), pp. 79–81.

[15] David Brydges, Jürg Fröhlich, and Thomas Spencer. "The random walk representation of classical spin systems and correlation inequalities". In: *Communications in Mathematical Physics* 83.1 (1982), pp. 123–150.

[16] Kurt Symanzik. *EUCLIDEAN QUANTUM FIELD THEORY*. Tech. rep. New York Univ., NY, 1969.

[17] Christina Goldschmidt, Daniel Ueltschi, and Peter Windridge. "Quantum Heisenberg models and their probabilistic representations". In: *Entropy and the quantum II, Contemp. Math* 552 (2011), pp. 177–224.

[18] Volker Betz and Daniel Ueltschi. "Spatial random permutations and Poisson-Dirichlet law of cycle lengths". In: (2011).

[19] Stefan Grosskinsky, Alexander A Lovisolo, and Daniel Ueltschi. "Lattice permutations and Poisson-Dirichlet distribution of cycle lengths". In: *Journal of Statistical Physics* 146.6 (2012), pp. 1105–1121.

[20] Adam Nahum et al. "Length distributions in loop soups". In: *Physical review letters* 111.10 (2013), p. 100601.

[21] Volker Betz. "Random permutations of a regular lattice". In: *Journal of Statistical Physics* 155 (2014), pp. 1222–1248.

[22] Alexandra Quitmann and Lorenzo Taggi. "Macroscopic loops in the Bose gas, Spin O (N) and related models". In: *Communications in Mathematical Physics* 400.3 (2023), pp. 2081–2136.

[23] Nicolas Forien et al. *Coexistence, enhancements and short loops in random walk loop soups*. 2023. arXiv: 2306.12102 [math.PR].

[24] PL Dobruschin. "The description of a random field by means of conditional probabilities and conditions of its regularity". In: *Theory of Probability & Its Applications* 13.2 (1968), pp. 197–224.

[25] Oscar E Lanford III and David Ruelle. "Observables at infinity and states with short range correlations in statistical mechanics". In: *Communications in Mathematical Physics* 13.3 (1969), pp. 194–215.

[26] Sacha Friedli and Yvan Velenik. *Statistical mechanics of lattice systems: a concrete mathematical introduction*. Cambridge University Press, 2017.

[27] Russell Lyons and Yuval Peres. *Probability on trees and networks*. Vol. 42. Cambridge University Press, 2017.

[28] Alexandra Quitmann and Lorenzo Taggi. "Macroscopic Loops in the Bose Gas, Spin O(N) and Related Models". In: *Communications in Mathematical Physics* 400.3 (Feb. 2023), pp. 2081–2136. ISSN: 1432-0916. DOI: 10.1007/s00220-023-04633-9. URL: http://dx.doi.org/10.1007/s00220-023-04633-9.

[29] Hugo Duminil-Copin. *Random currents expansion of the Ising model*. 2017. arXiv: 1607.06933 [math-ph].

[30] W. K. Hastings. "Monte Carlo Sampling Methods using Markov Chains and their Applications". In: *Biometrika* 57.1 (Apr. 1970), pp. 97–109. DOI: 10.1093/biomet/57.1.97.

[31] Roy J. Glauber. "Time-Dependent Statistics of the Ising Model". In: *Journal of Mathematical Physics* 4.2 (Feb. 1963), pp. 294–307. ISSN: 0022-2488. DOI: 10.1063/1.1703954. eprint: https://pubs.aip.org/aip/jmp/article-pdf/4/2/294/19156949/294_1_online.pdf. URL: https://doi.org/10.1063/1.1703954.

[32] J. R. Norris. *Markov Chains*. Cambridge Series in Statistical and Probabilistic Mathematics. Cambridge University Press, 1997.

[33] Andrew Gelman and Donald B Rubin. "Inference from iterative simulation using multiple sequences". In: *Statistical Science* 7.4 (1992), pp. 457–472.

[34] Ravin Kumar et al. "ArviZ a unified library for exploratory analysis of Bayesian models in Python". In: *Journal of Open Source Software* 4.33 (2019), p. 1143. DOI: 10.21105/joss.01143. URL: https://doi.org/10.21105/joss.01143.

[35] Martin Hasenbusch. "The two-dimensional XY model at the transition temperature: a high-precision Monte Carlo study". In: *Journal of Physics A: Mathematical and General* 38.26 (2005), p. 5869.

[36] Fumiko Yonezawa, Shoichi Sakamoto, and Motoo Hori. "Percolation in two-dimensional lattices. I. A technique for the estimation of thresholds". In: *Phys. Rev. B* 40 (1 July 1989), pp. 636–649. DOI: 10.1103/PhysRevB.40.636. URL: https://link.aps.org/doi/10.1103/PhysRevB.40.636.